Observational Evidence of Increased Afternoon Rainfall Downwind of Irrigated Areas

P.Greve[1], A. U. Schmitt[1], D. G. Miralles[2], S. McDermid[3,4], K. L. Findell[5], A. García-García[6], J. Peng[6,7]

1: Helmholtz-Zentrum Hereon, Hamburg, Germany
2: Hydro-Climate Extremes Lab, Ghent University, Belgium
3: Department of Environmental Studies, New York University, USA
4: NASA Goddard Institute for Space Studies, New York, USA
5: Geophysical Fluid Dynamics Laboratory (GFDL), NOAA, Princeton, USA
6: Department of Remote Sensing, UFZ, Leipzig, Germany
7: Institute for Earth System Science and Remote Sensing, Leipzig University, Germany

Publication

UWaRes

Helmholtz-Zentrum hereon

GHENT UNIVERSITY

NOAA

GERICS Climate Service Center Germany

Eine Einrichtung des Helmholtz-Zentrums Hereon

NASA

UFZ

Uncertain Water Resources

UWaRes

Helmholtz-Zentrum hereon

CWatM

Climate Model

Atmosphere

Precipitation, Temperature, Wind speed, Radiation, Humidity, Surface Pressure

CWatM

Land surface

Evaporation, Vegetation, Land cover, Soils, Snow

River Routing

Water Management

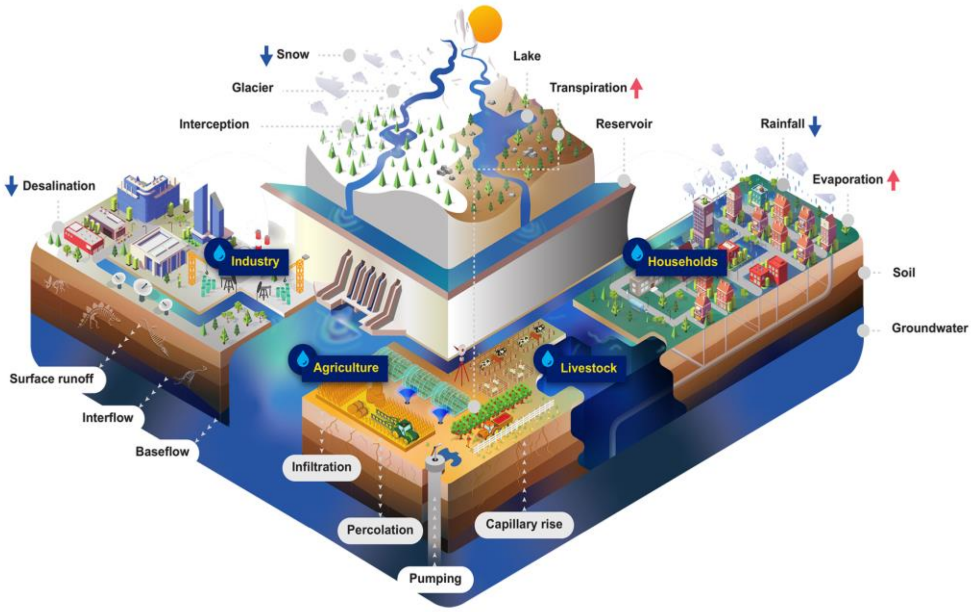

Water Availability

Sectoral Water Demand

CWatM

Community Water Model

- large-scale rainfall runoff and channel routing water resources model

- Spatial resolution:
  0.5°, 0.5′, (1km)
- Temporal resolution:
  daily

CWatM

Climate Model

Atmosphere

Precipitation, Temperature, Wind speed, Radiation, Humidity, Surface Pressure

CWatM

Land surface

Evaporation, Vegetation, Land cover, Soils, Snow

River Routing

Water Management

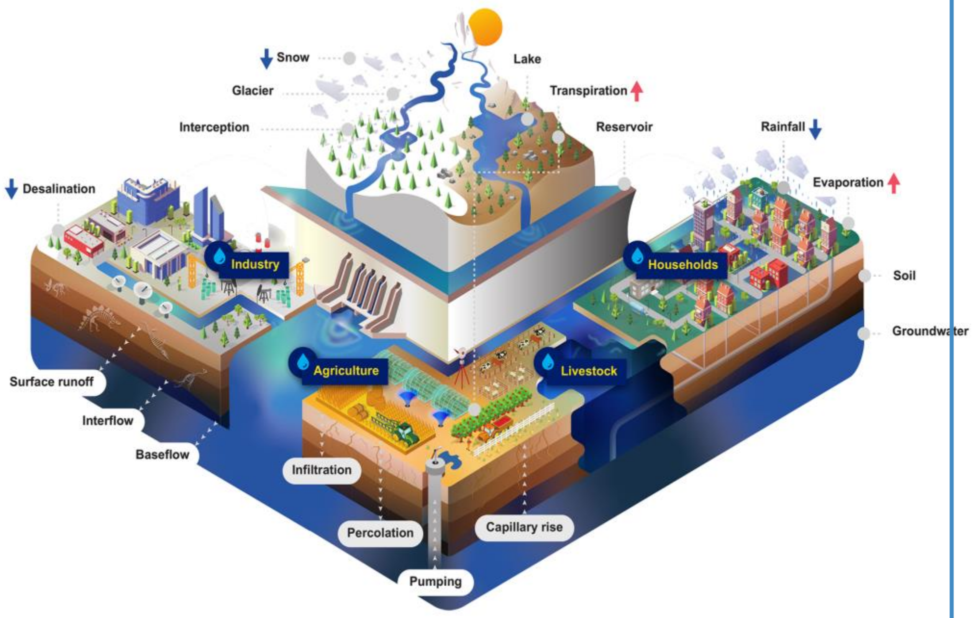

Water Availability

Sectoral Water Demand

Water withdrawals

- industry
- livestock
- irrigation
- households
- environmental need

Irrigation in RCMs

Regional rainfall

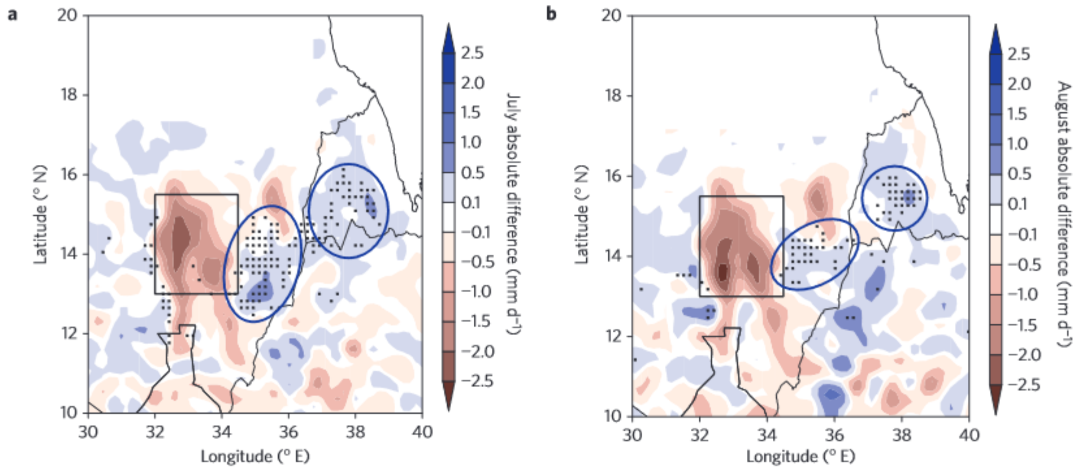

Alter et al., *Nat. Geosci.*, 2015

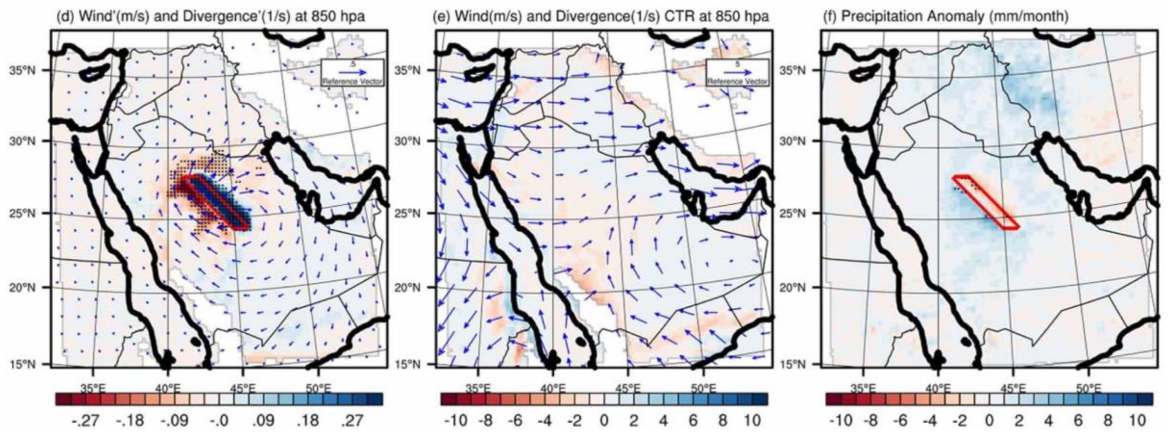

Lo et al., *ERL*, 2021

Convection-permitting simulations

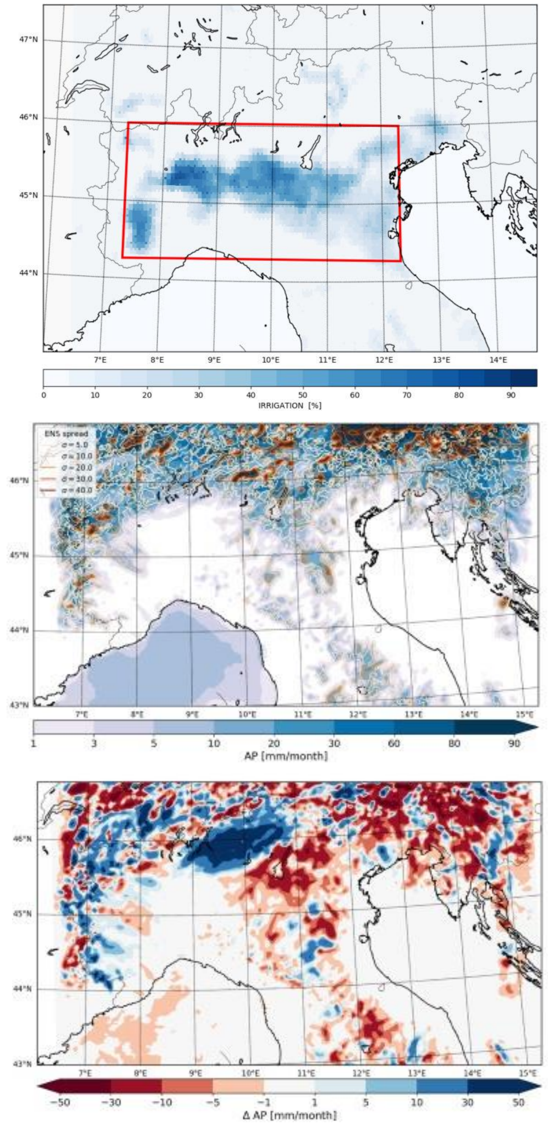

Valmassoi et al., *AR*, 2020

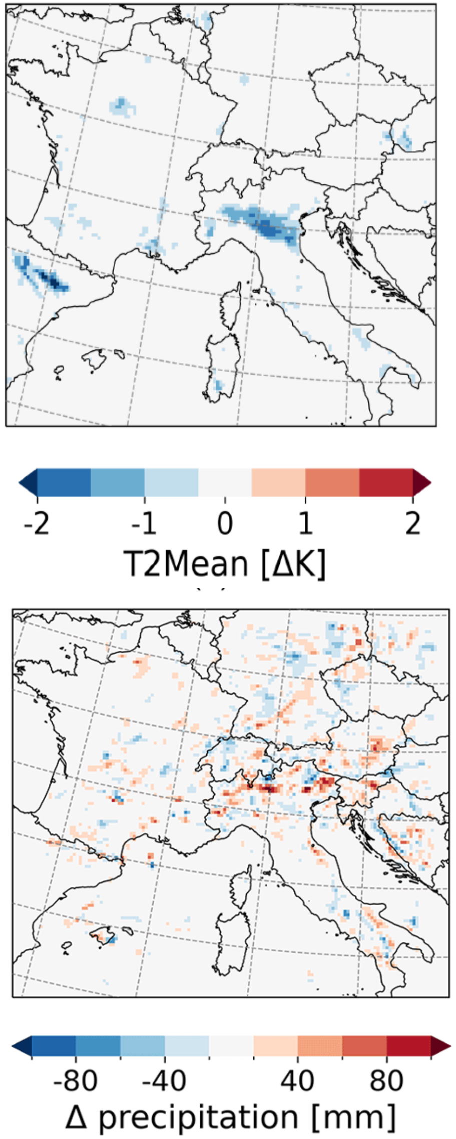

Asmus et al., *GMD*, 2023

CWatM

C-CWatM

Climate Model

Atmosphere

Precipitation, Temperature, Wind speed, Radiation, Humidity, Surface Pressure

CWatM

Land surface

Evaporation, Vegetation, Land cover, Soils, Snow

River Routing

Water Management

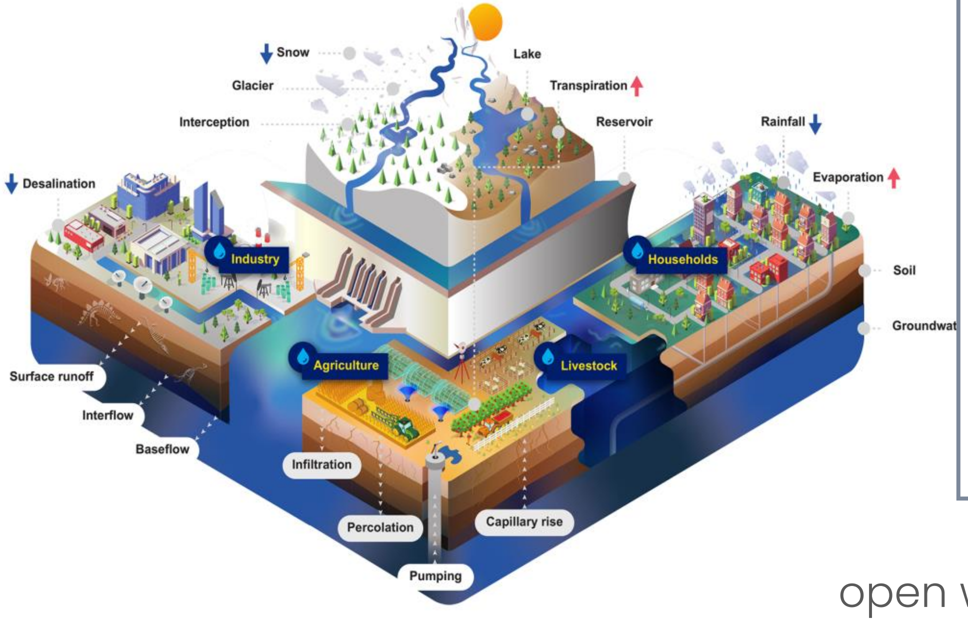

Water Availability

Sectoral Water Demand

Climate Model

Atmosphere

Precipitation, Temperature, Wind speed, Radiation, Humidity, Surface Pressure

Land surface

Evaporation, Vegetation, Land cover, Soils, Snow

Runoff
open water evap

Soil moisture
drainage

C-CWatM

River Routing

Water Management

Irrigation in RCMs

Regional rainfall

Alter et al., *Nat. Geosci.*, 2015

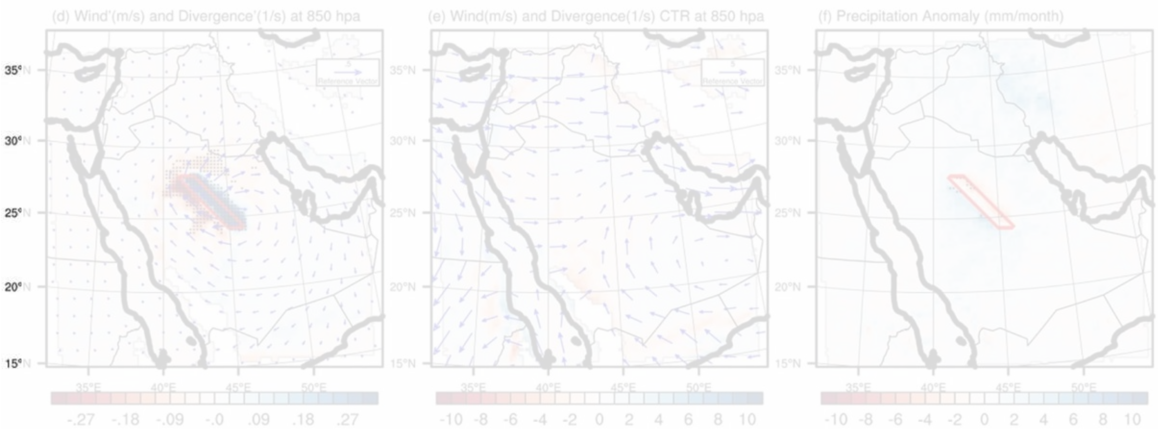

Lo et al., *ERL*, 2021

Convection-permitting simulations

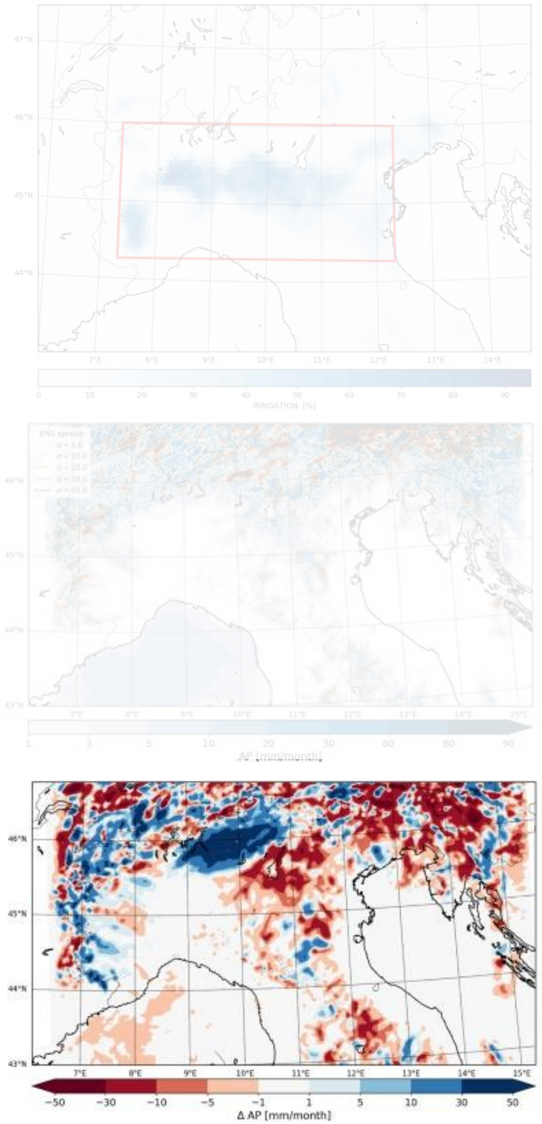

Valmassoi et al., *AR*, 2020

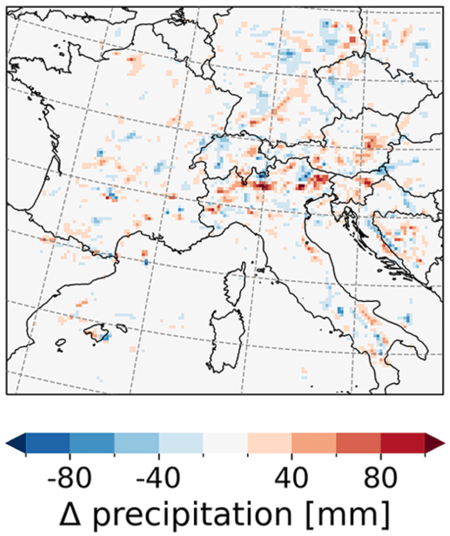

Asmus et al., *GMD*, 2023

Irrigation in RCMs

Regional rainfall

nature geoscience

Explore content ˅ About the journal ˅ Publish with us ˅

nature › nature geoscience › letters › article

Letter | Published: 05 June 2011

Probability of afternoon precipitation in eastern United States and Mexico enhanced by high evaporation

Kirsten L. Findell ✉, Pierre Gentine, Benjamin R. Lintner & Christopher Kerr

Nature Geoscience 4, 434–439 (2011) | Cite this article

nature communications

Explore content ˅ About the journal ˅ Publish with us ˅

nature › nature communications › articles › article

Article | Open access | Published: 05 March 2015

Reconciling spatial and temporal soil moisture effects on afternoon rainfall

Benoit P. Guillod ✉, Boris Orlowsky, Diego G. Miralles, Adriaan J. Teuling & Sonia I. Seneviratne

Nature Communications 6, Article number: 6443 (2015) | Cite this article

nature

Explore content ˅ About the journal ˅ Publish with us ˅

nature › letters › article

Letter | Published: 12 September 2012

Afternoon rain more likely over drier soils

Christopher M. Taylor ✉, Richard A. M. de Jeu, Françoise Guichard, Phil P. Harris & Wouter A. Dorigo

Nature 489, 423–426 (2012) | Cite this article

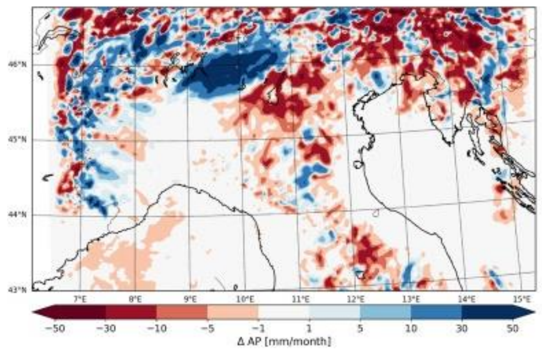

Valmassoi et al., *AR*, 2020

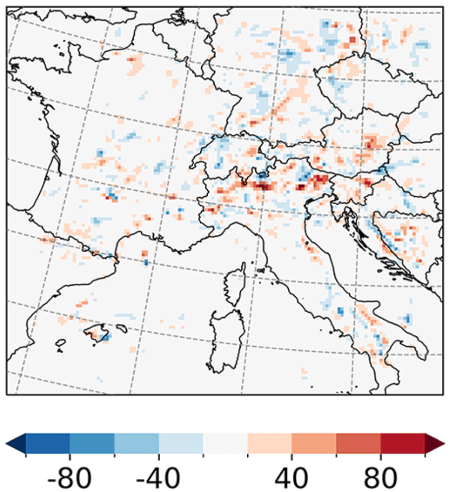

Asmus et al., *GMD*, 2023

Irrigation

Uncertain impact on local/regional rainfall

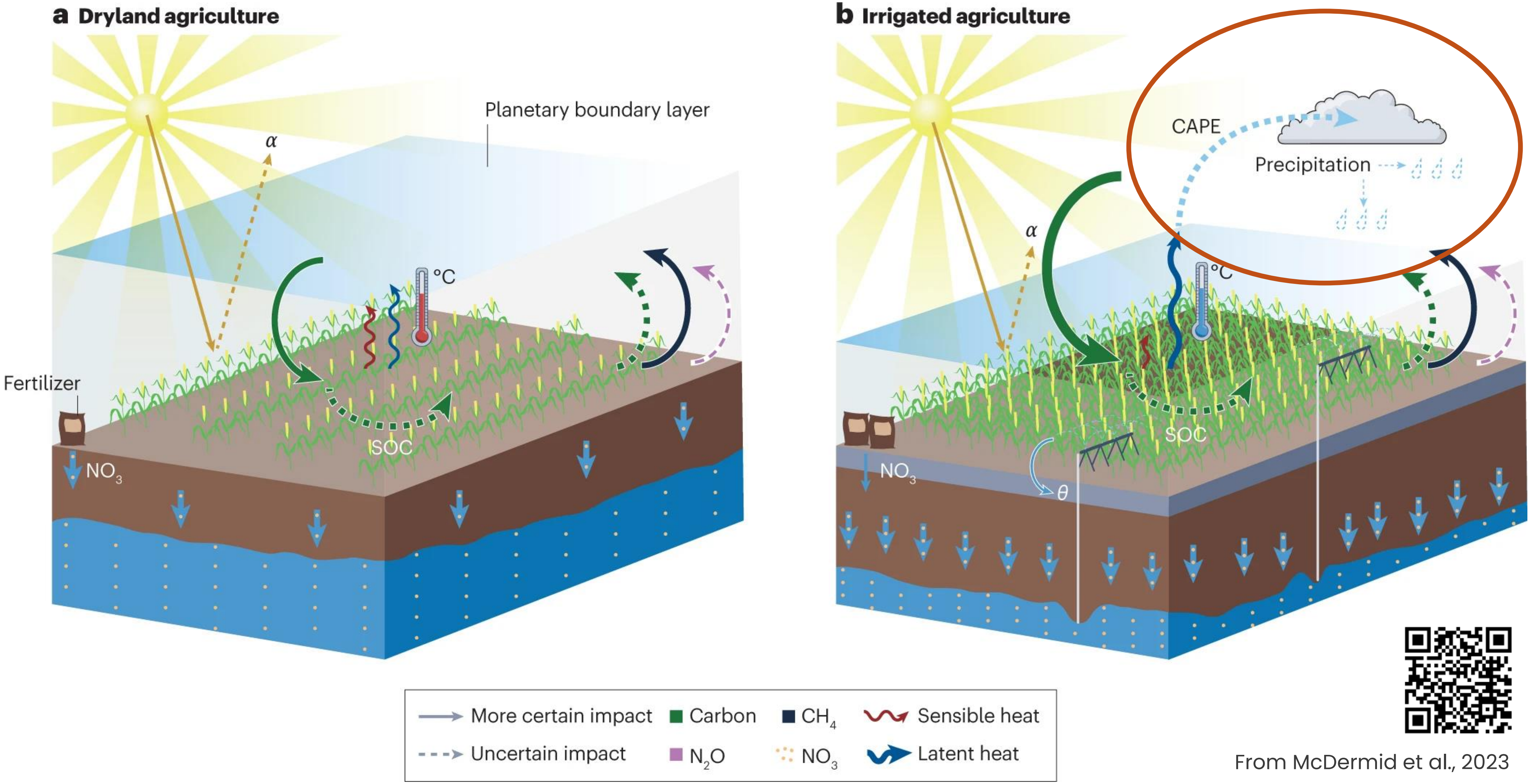

From McDermid et al., 2023

Irrigation

Global irrigated areas, AQUASTAT, FAO

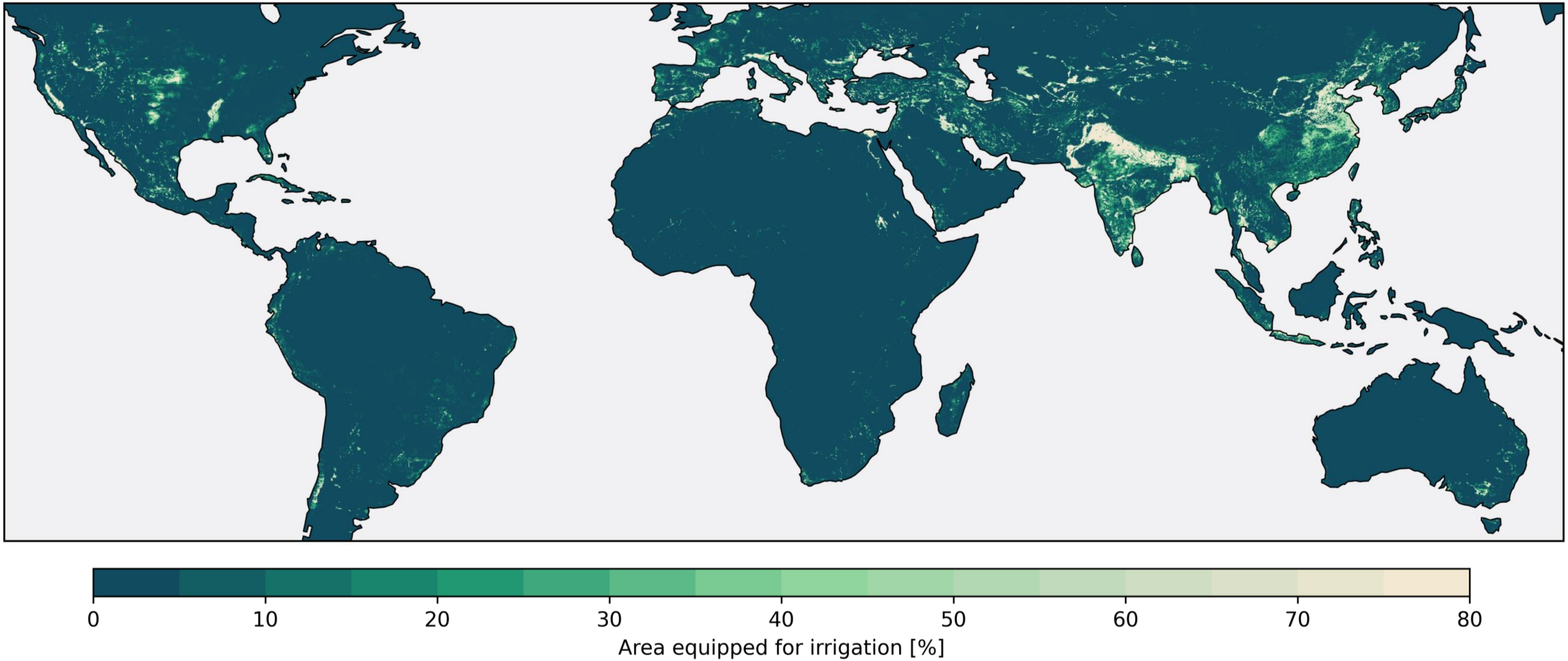

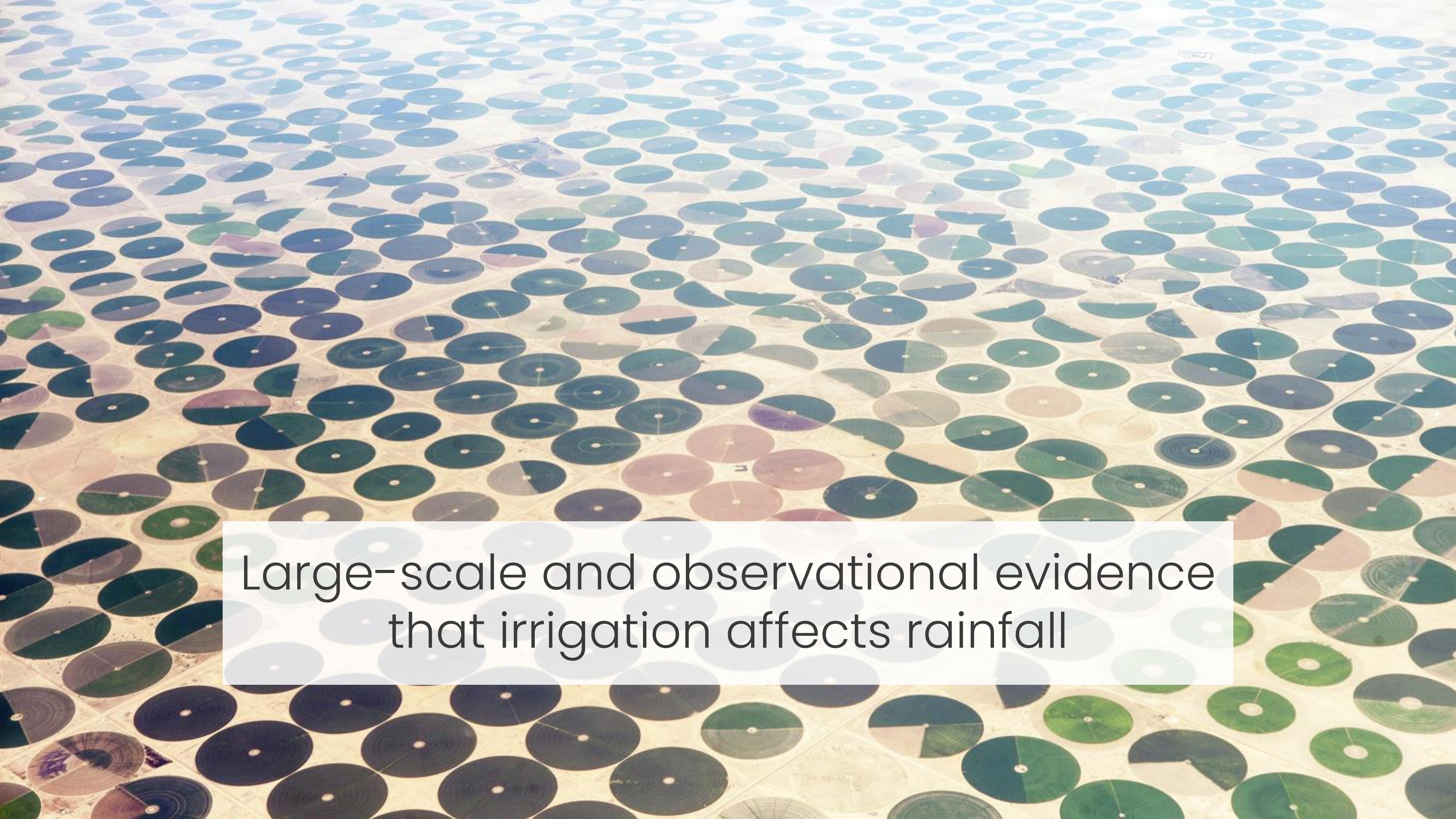

Large-scale and observational evidence that irrigation affects rainfall

Afternoon rain

- Percentage area equipped for irrigation (AQUASTAT, FAO)
- High-resolution (0.1deg), sub-daily precipitation datasets (MSWEP, IMERG)

Afternoon rain

- Percentage area equipped for irrigation (AQUASTAT, FAO)
- High-resolution (0.1deg), sub-daily precipitation datasets (MSWEP, IMERG)

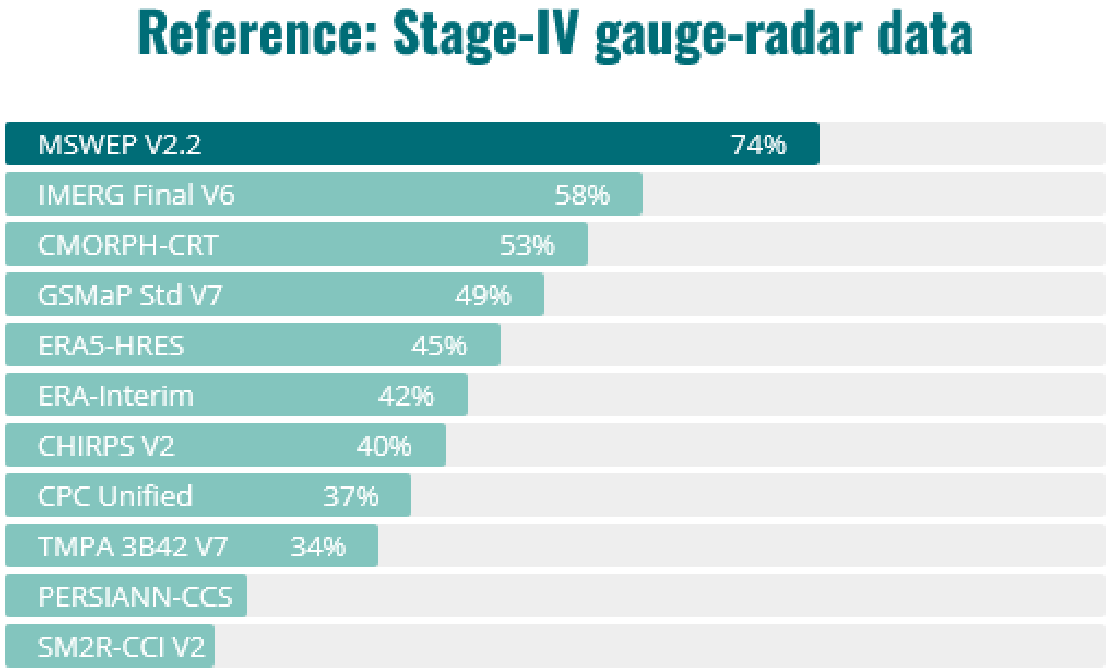

Values represent the mean daily temporal R^2 over the US
Adapted from Beck et al. (2019)

Afternoon rain

- Percentage area equipped for irrigation (AQUASTAT, FAO)
- High-resolution (0.1deg), sub-daily precipitation datasets (MSWEP, IMERG)

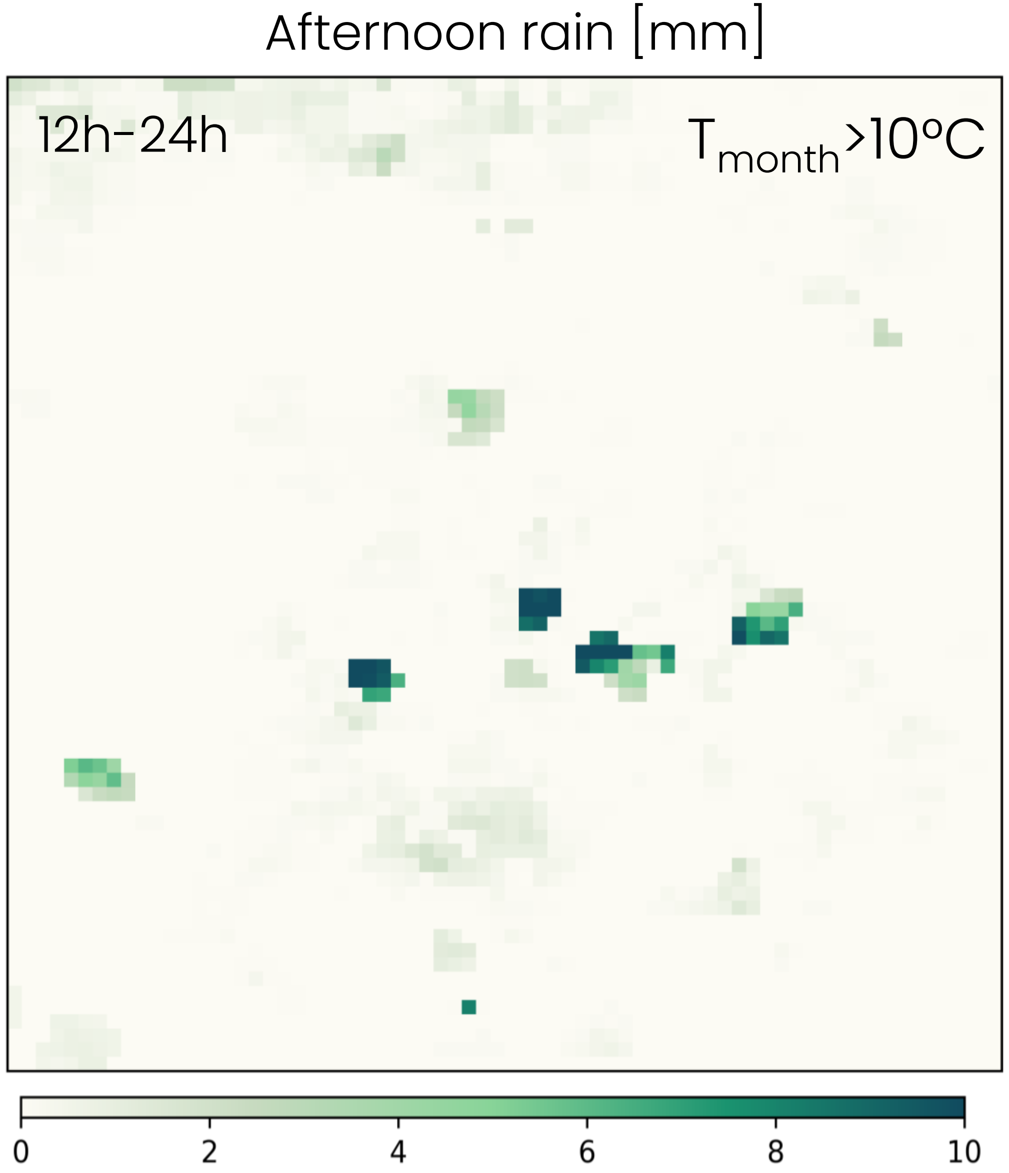

Afternoon rain

- Percentage area equipped for irrigation (AQUASTAT, FAO)
- High-resolution (0.1deg), sub-daily precipitation datasets (MSWEP, IMERG)

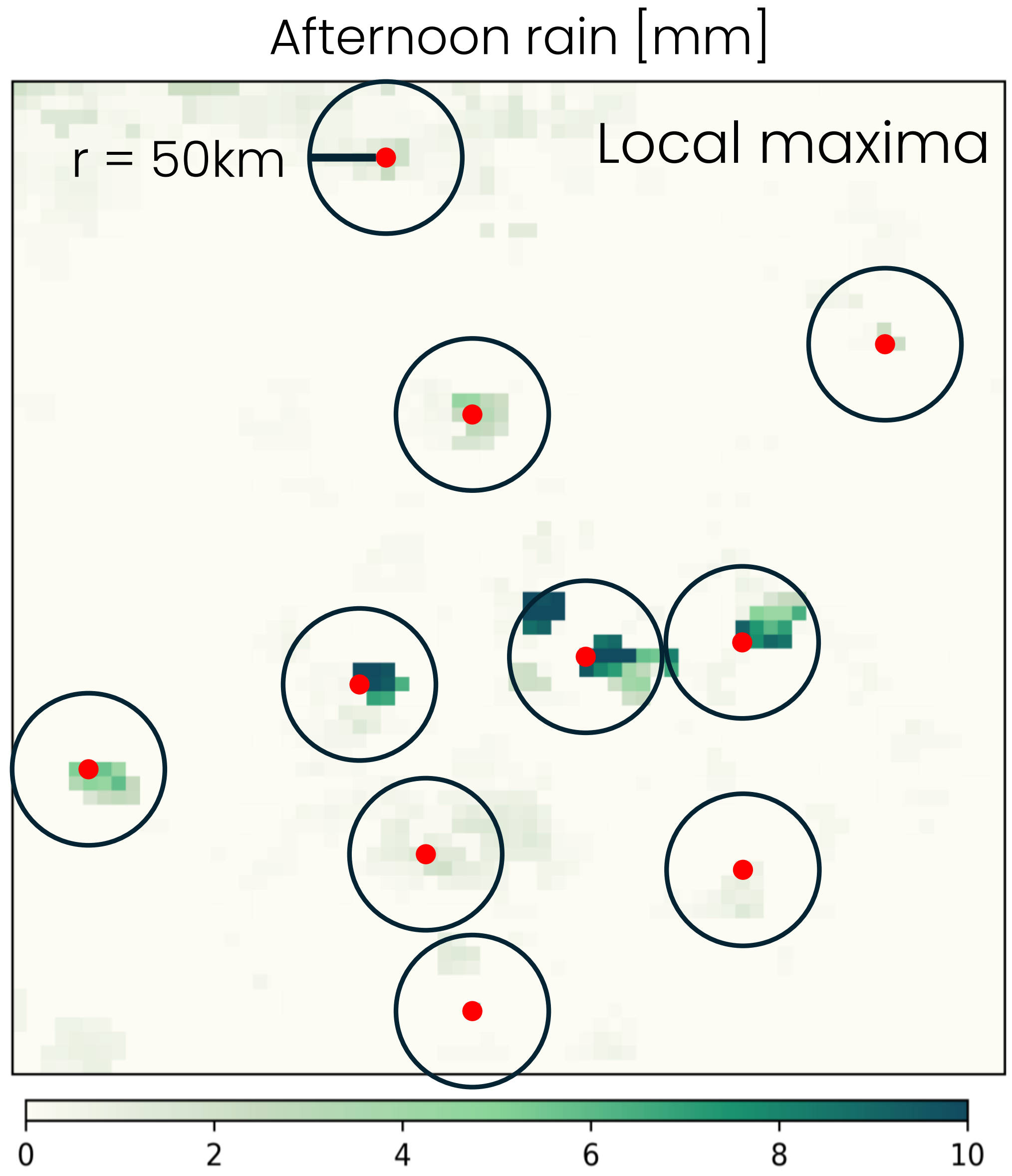

Afternoon rain

- Percentage area equipped for irrigation (AQUASTAT, FAO)
- High-resolution (0.1deg), sub-daily precipitation datasets (MSWEP, IMERG)

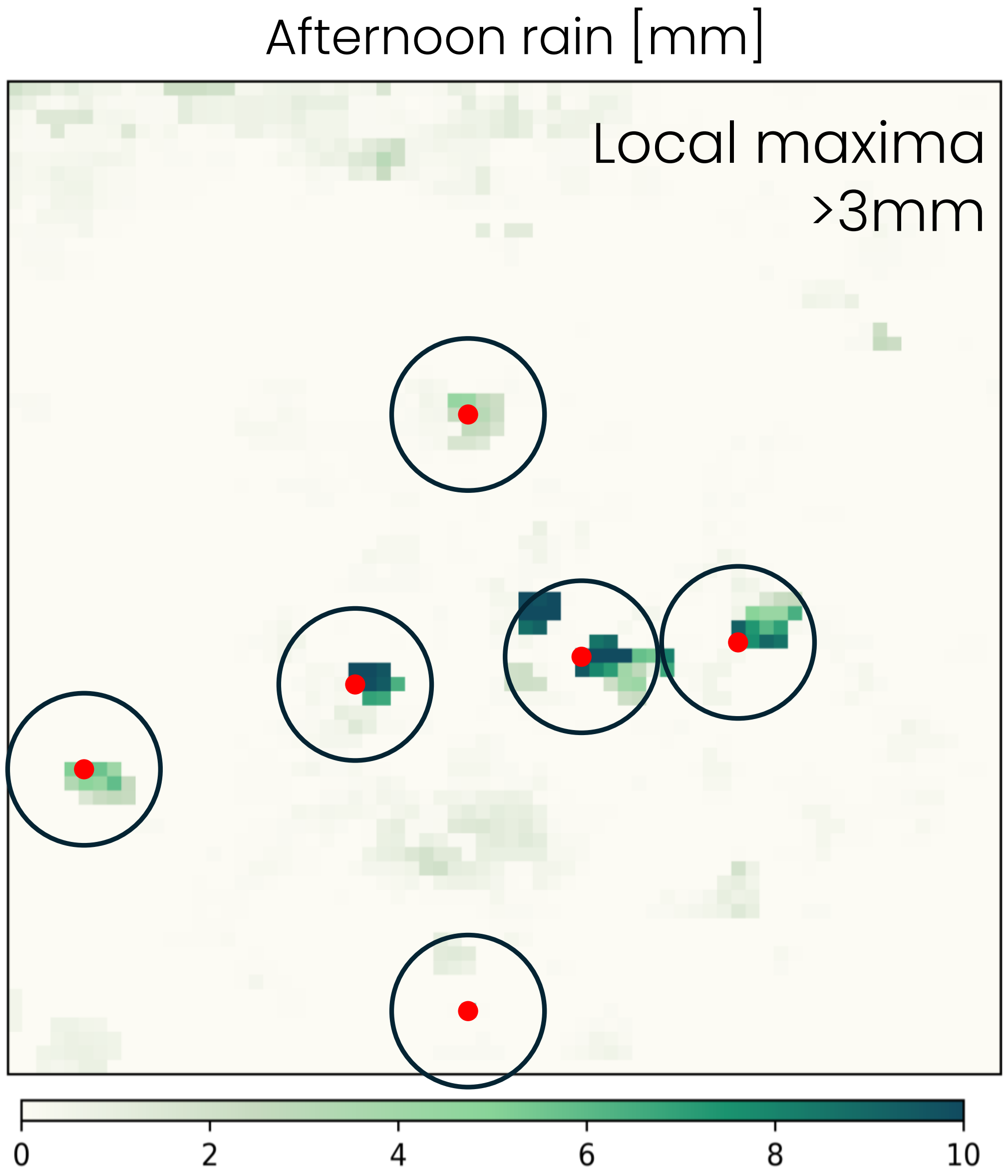

Afternoon rain

- Percentage area equipped for irrigation (AQUASTAT, FAO)
- High-resolution (0.1deg), sub-daily precipitation datasets (MSWEP, IMERG)

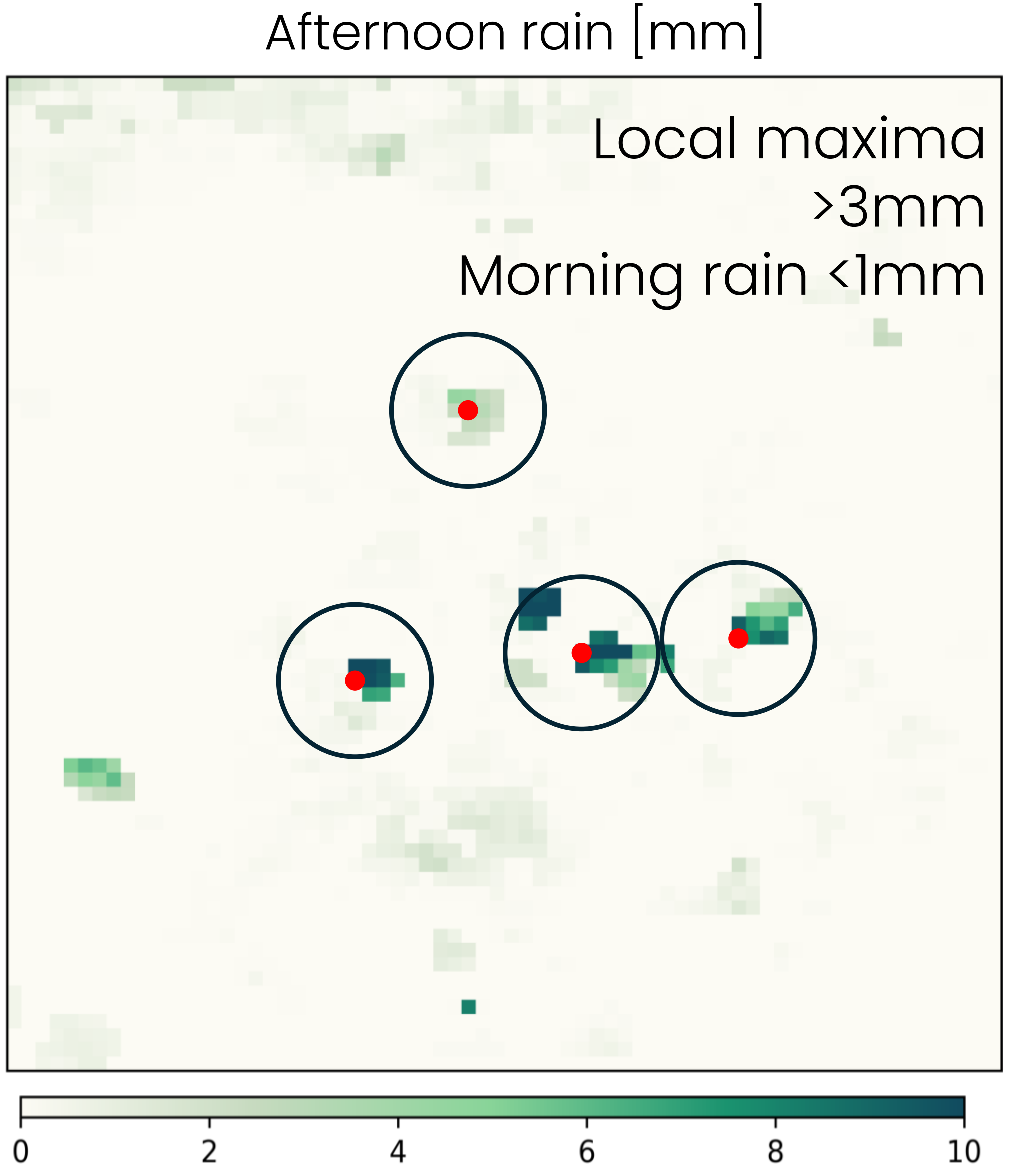

Afternoon rain

- Percentage area equipped for irrigation (AQUASTAT, FAO)
- High-resolution (0.1deg), sub-daily precipitation datasets (MSWEP, IMERG)

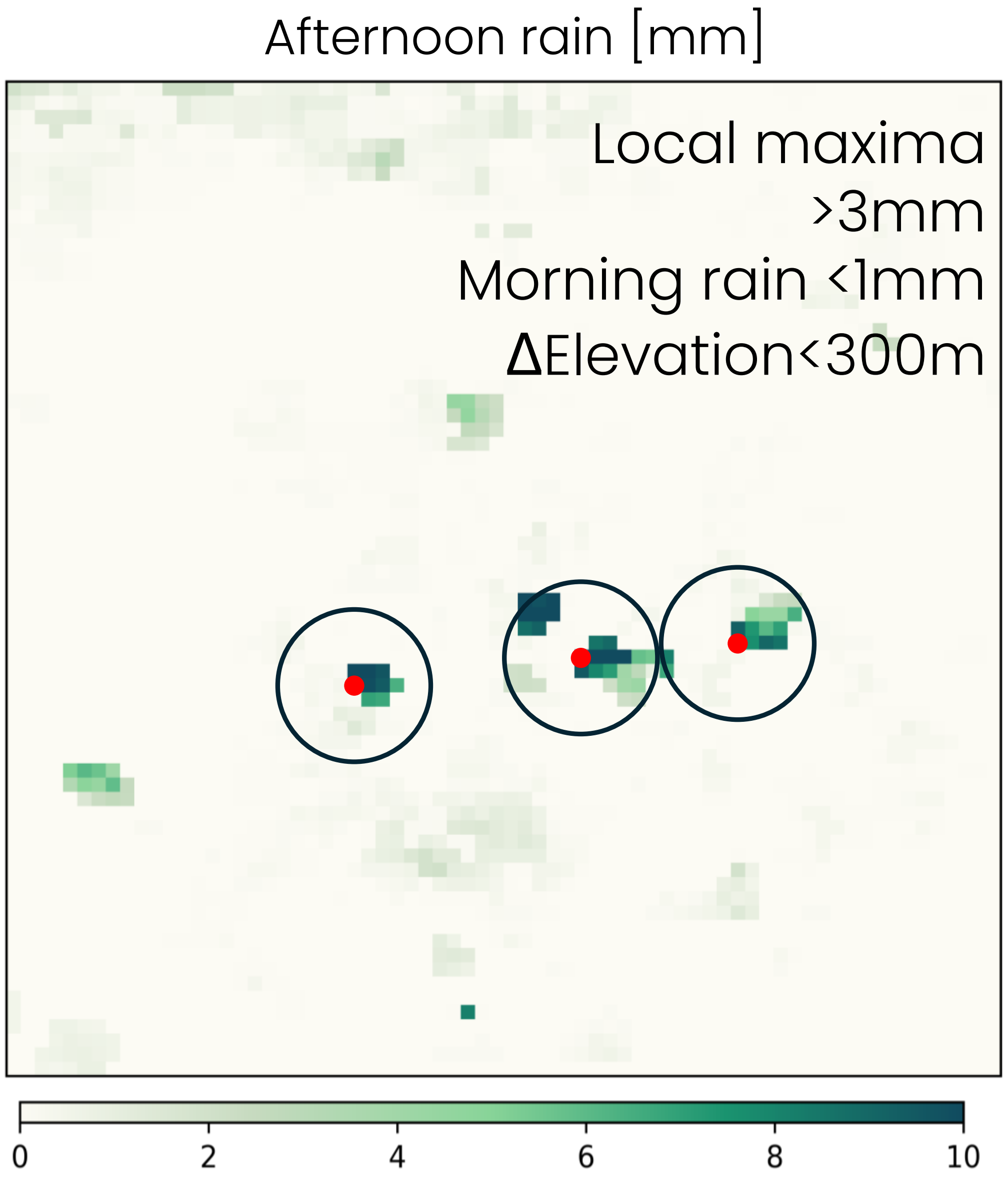

Afternoon rain

- Percentage area equipped for irrigation (AQUASTAT, FAO)
- High-resolution (0.1deg), sub-daily precipitation datasets (MSWEP, IMERG)

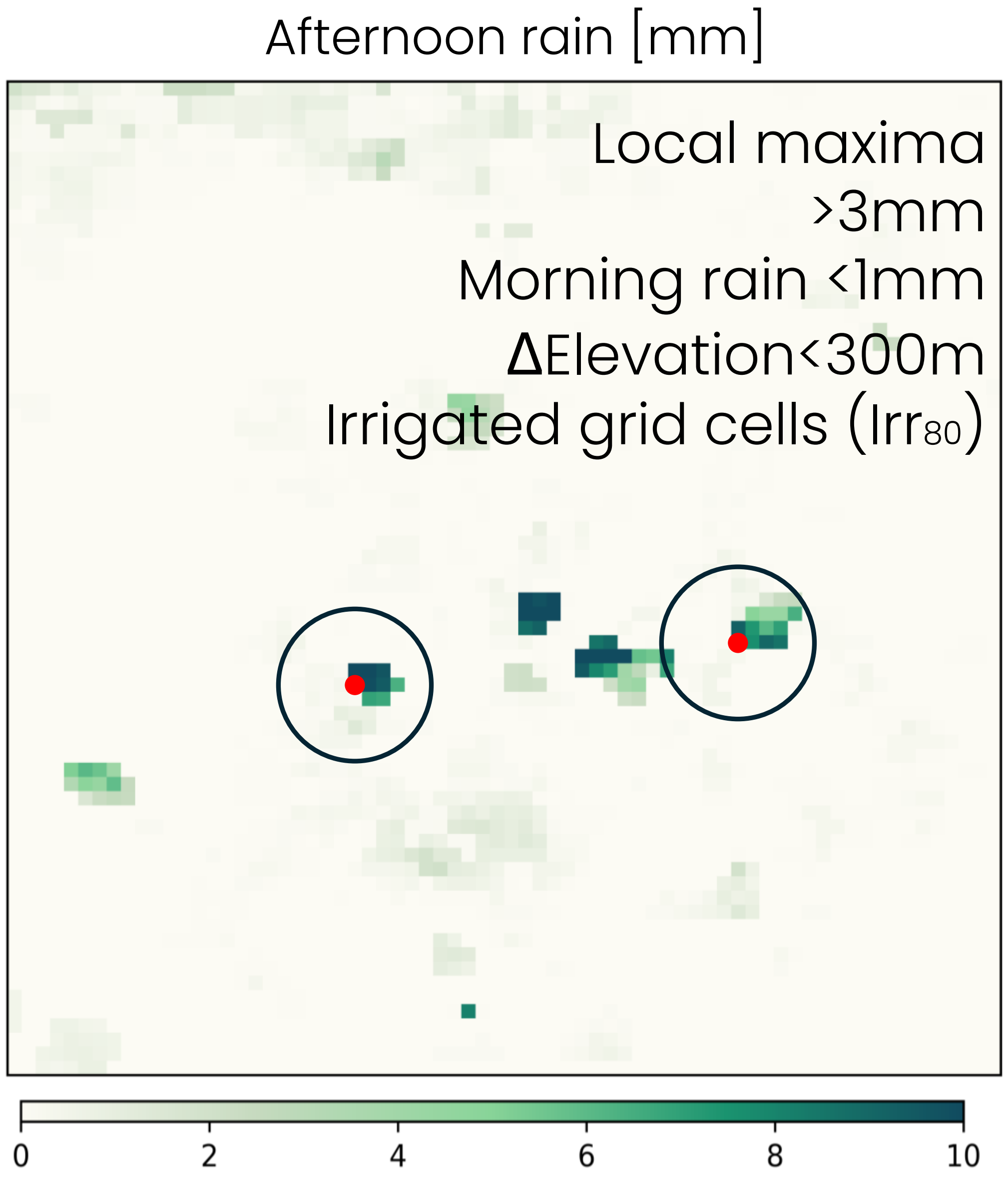

Afternoon rain

These criteria are used to select individual **afternoon rain** events most likely **triggered by local meteorological conditions** instead of other factors, such as synoptic-scale and orographic mechanisms

Afternoon rain

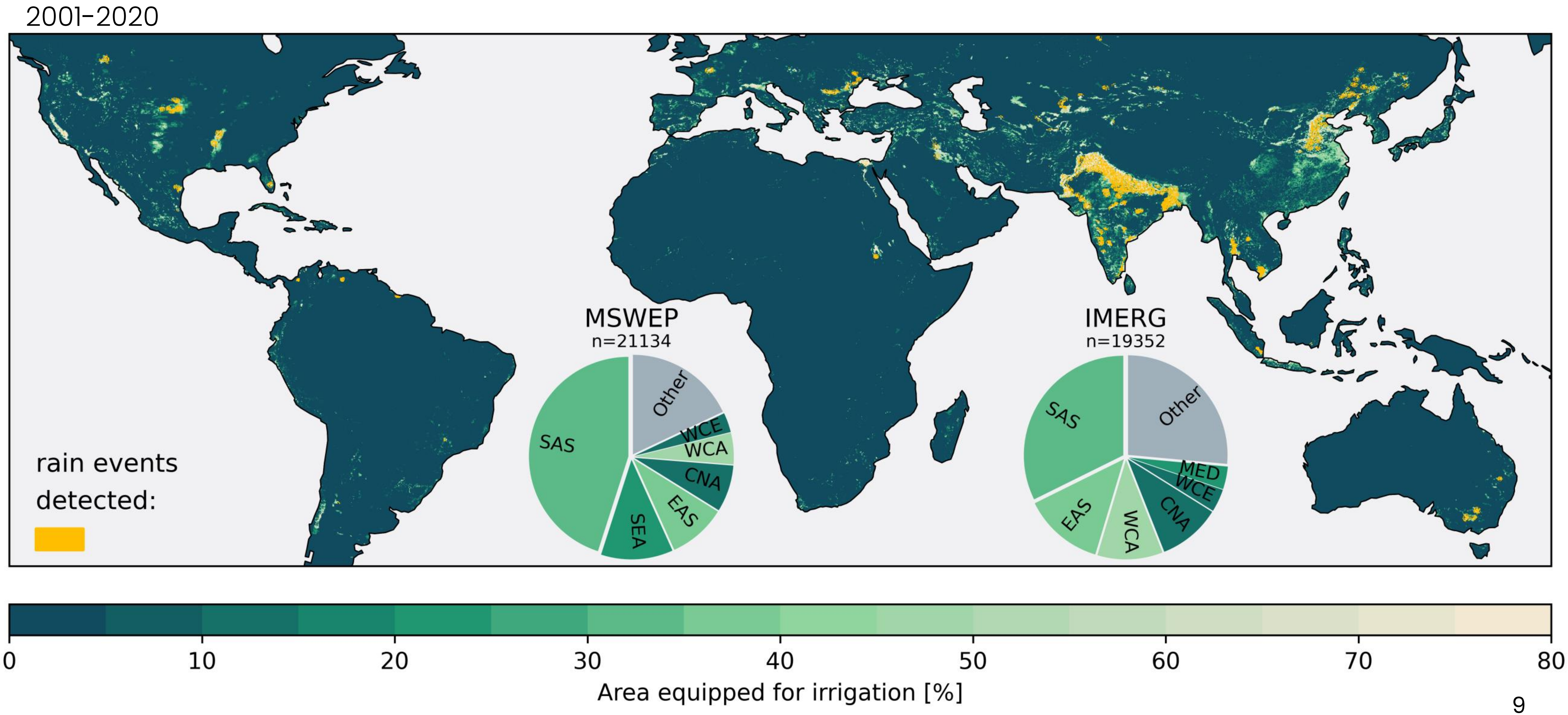

Afternoon rain

Fraction of irrigated grid cells per event

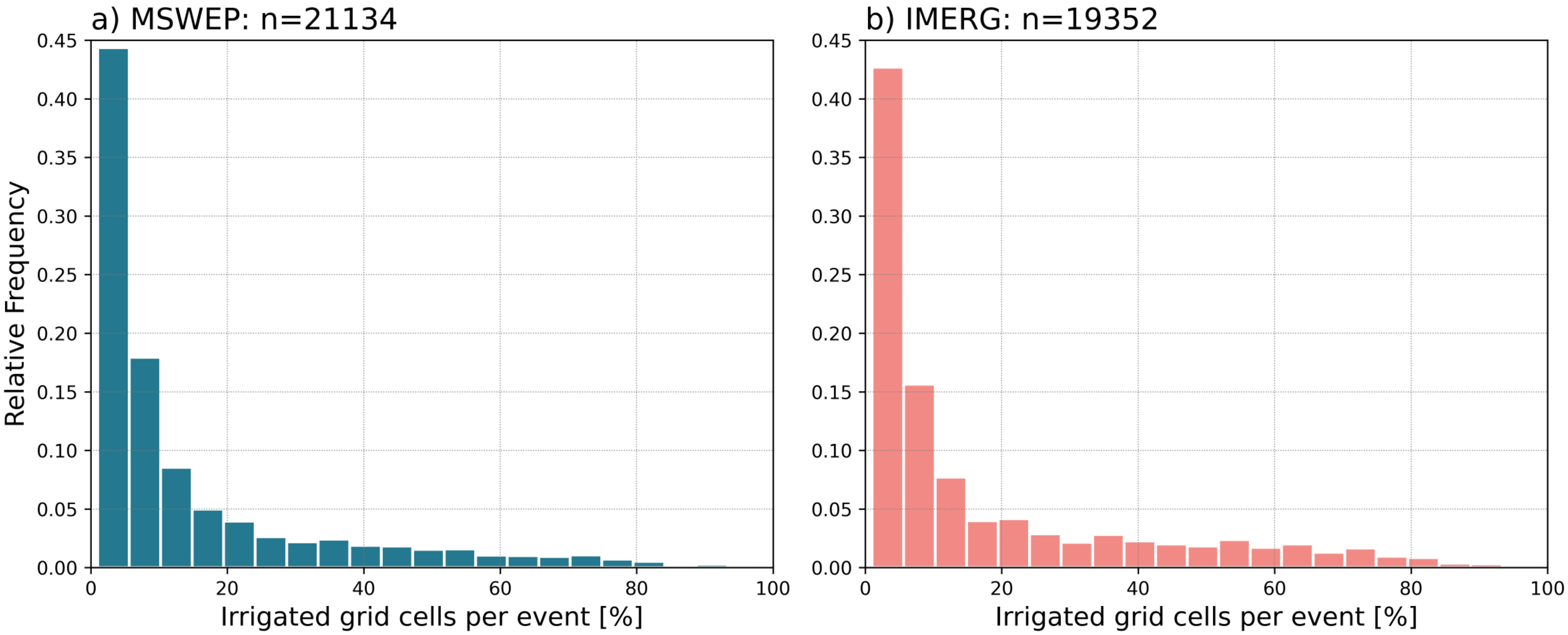

Afternoon rain

- Percentage area equipped for irrigation (AQUASTAT, FAO)
- High-resolution (0.1deg), sub-daily precipitation datasets (MSWEP, IMERG)

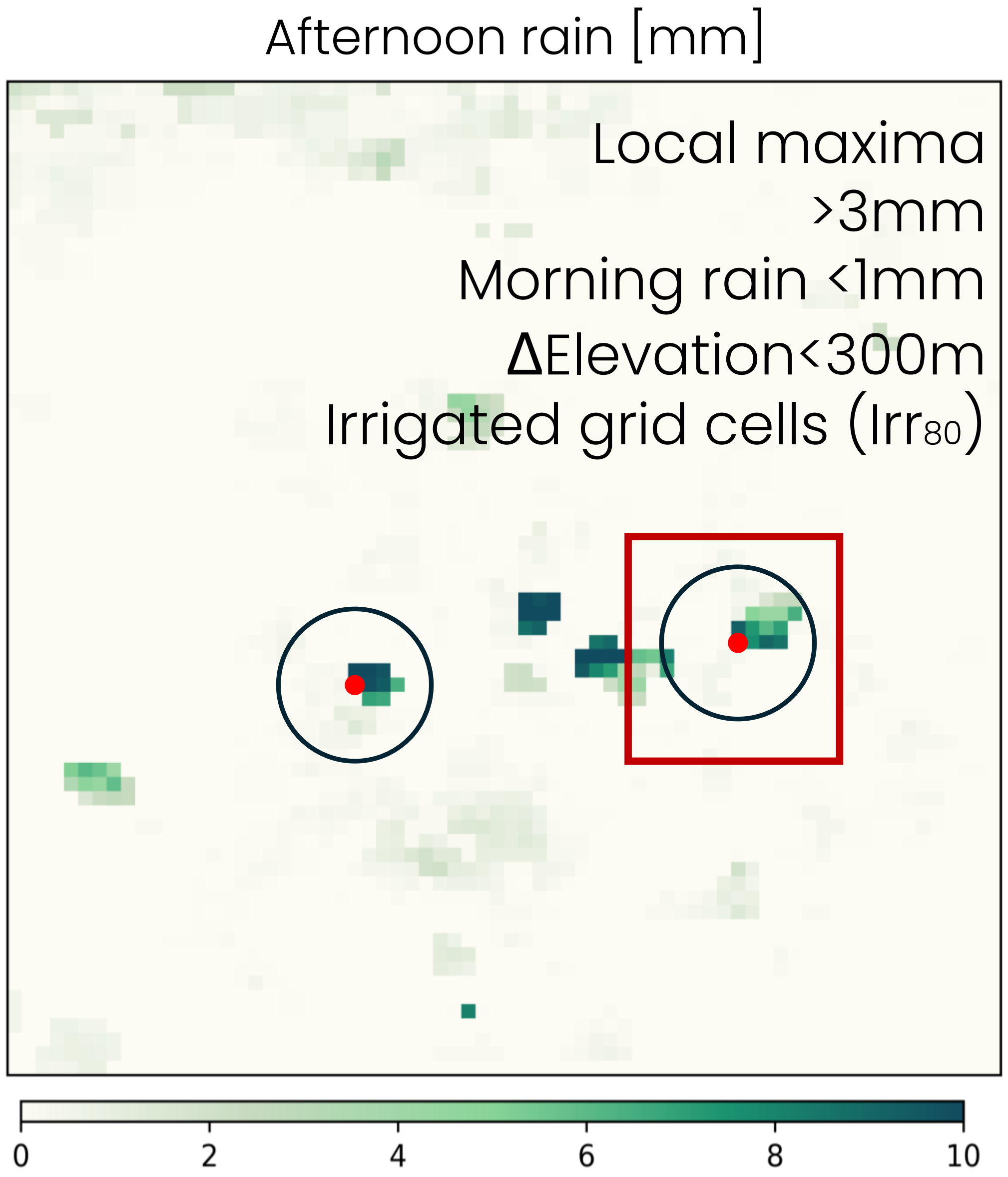

Afternoon rain

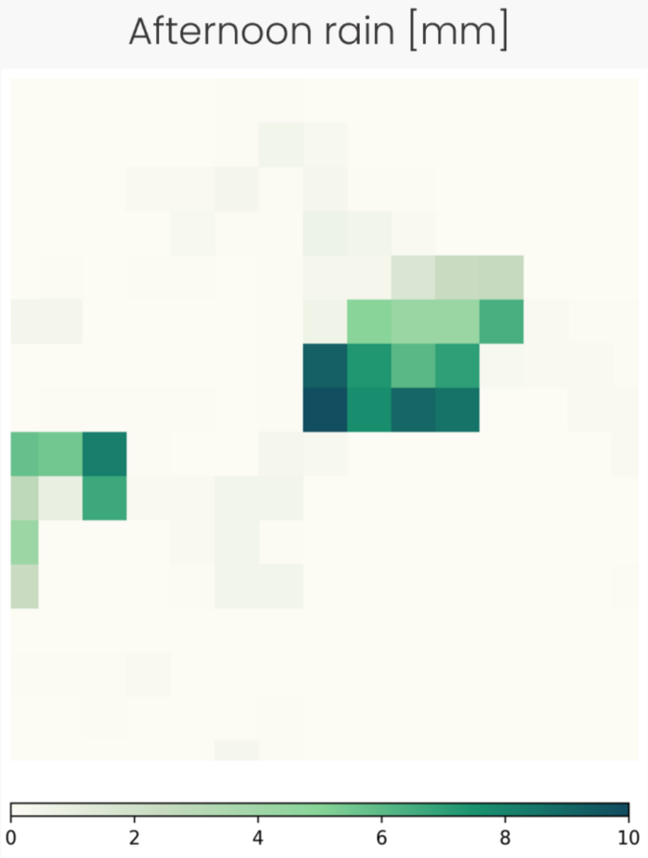

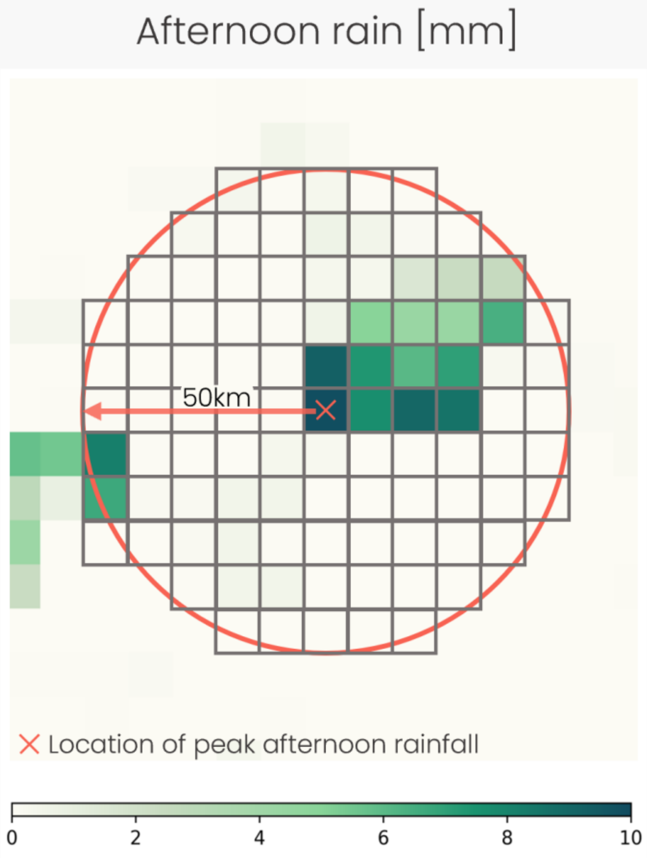

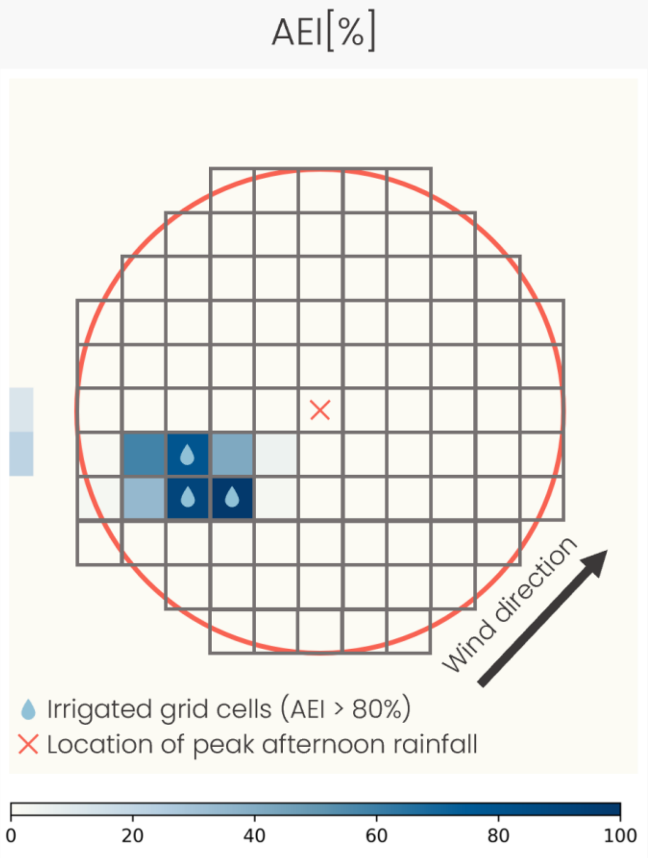

1. Compute the total amount of **daily afternoon rain** between 12h and 24h local time

2. Find **local rain maxima** (> 3mm) within a **50km radius** around the peak location

3. Consider only rain events where: **ΔElevation <300m** **Morning rain < 1mm** T_{mon} > 10°C

4. Consider only rain events near both **irrigated** (AEI>80%) and **non-irrigated** grid cells

5. **Transformation** toward a **wind-based** and irrigation-centred reference system

Afternoon rain event

- Percentage area equipped for irrigation (AQUASTAT, FAO)
- High-resolution (0.1deg), sub-daily precipitation datasets (MSWEP, IMERG)
- ERA5 wind vector analysis (monthly)

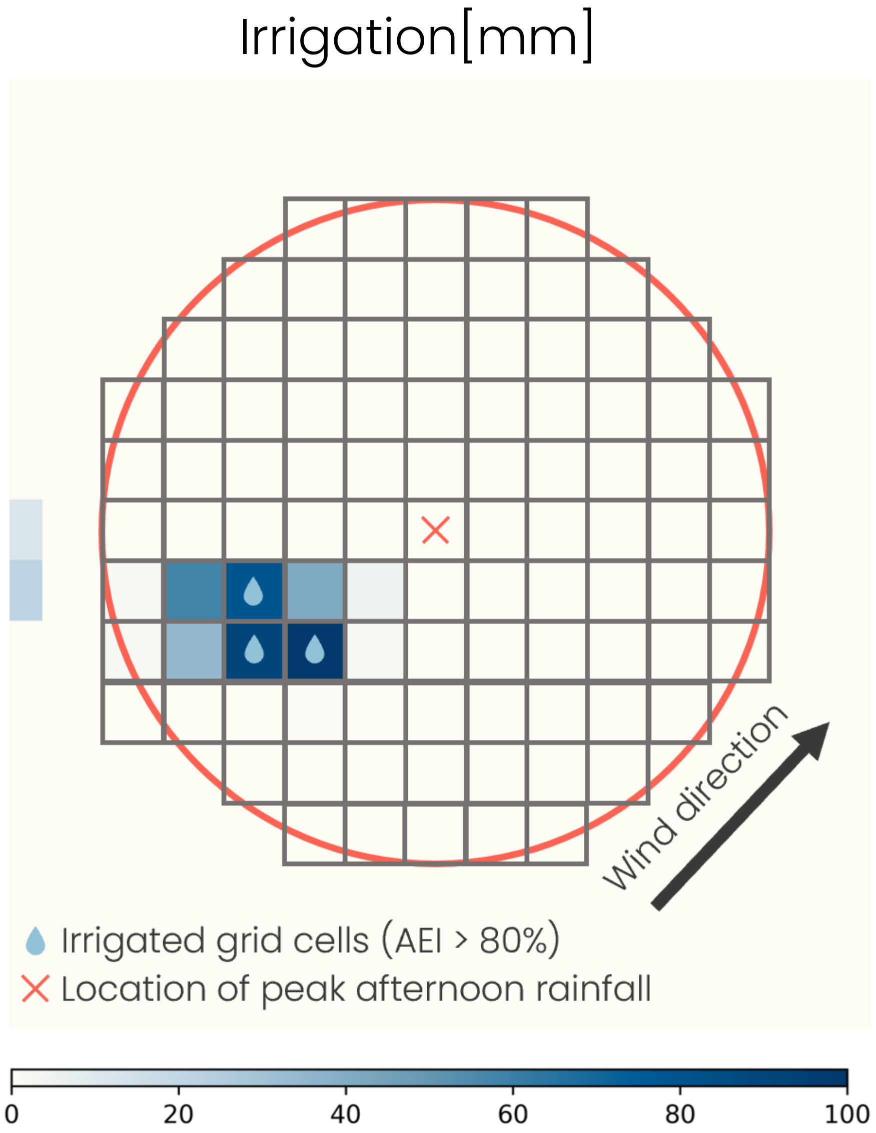

Irrigation and afternoon rain

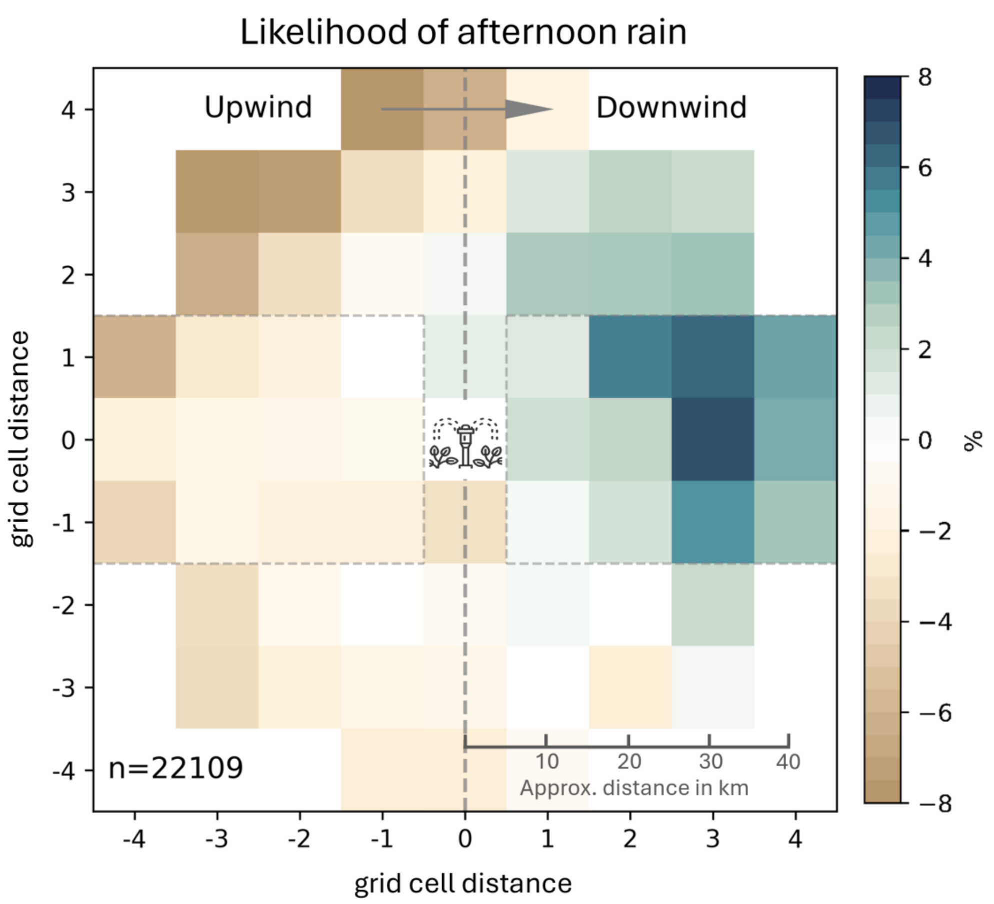

- Large-scale **irrigation enhances** the likelihood of **afternoon rain** 10km to 50km **downwind** of irrigated areas

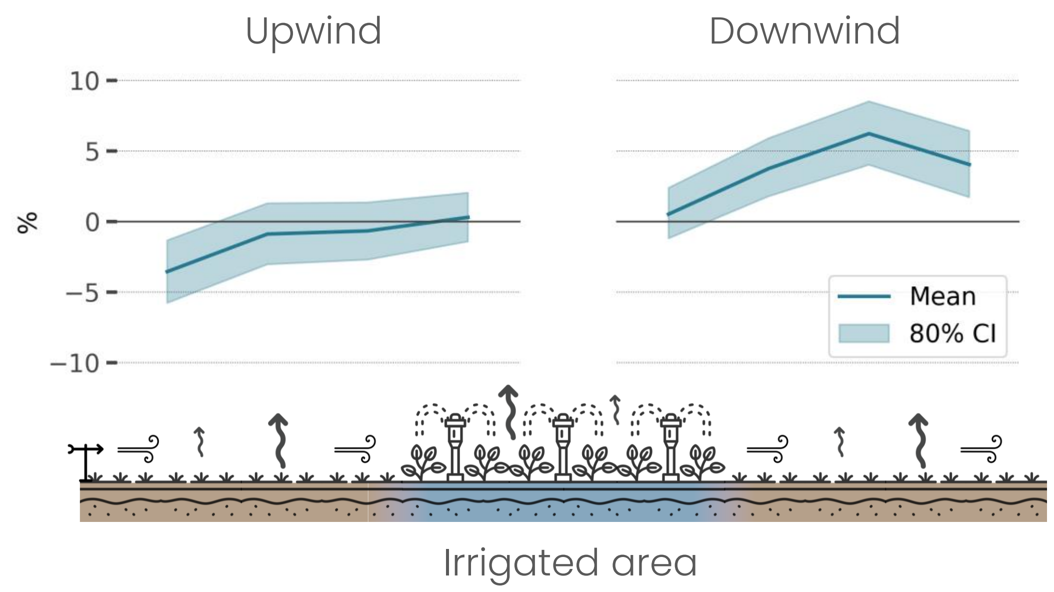

Afternoon rainfall likelihood

- Enhanced likelihood of afternoon rain 10km to 50km downwind of irrigated areas

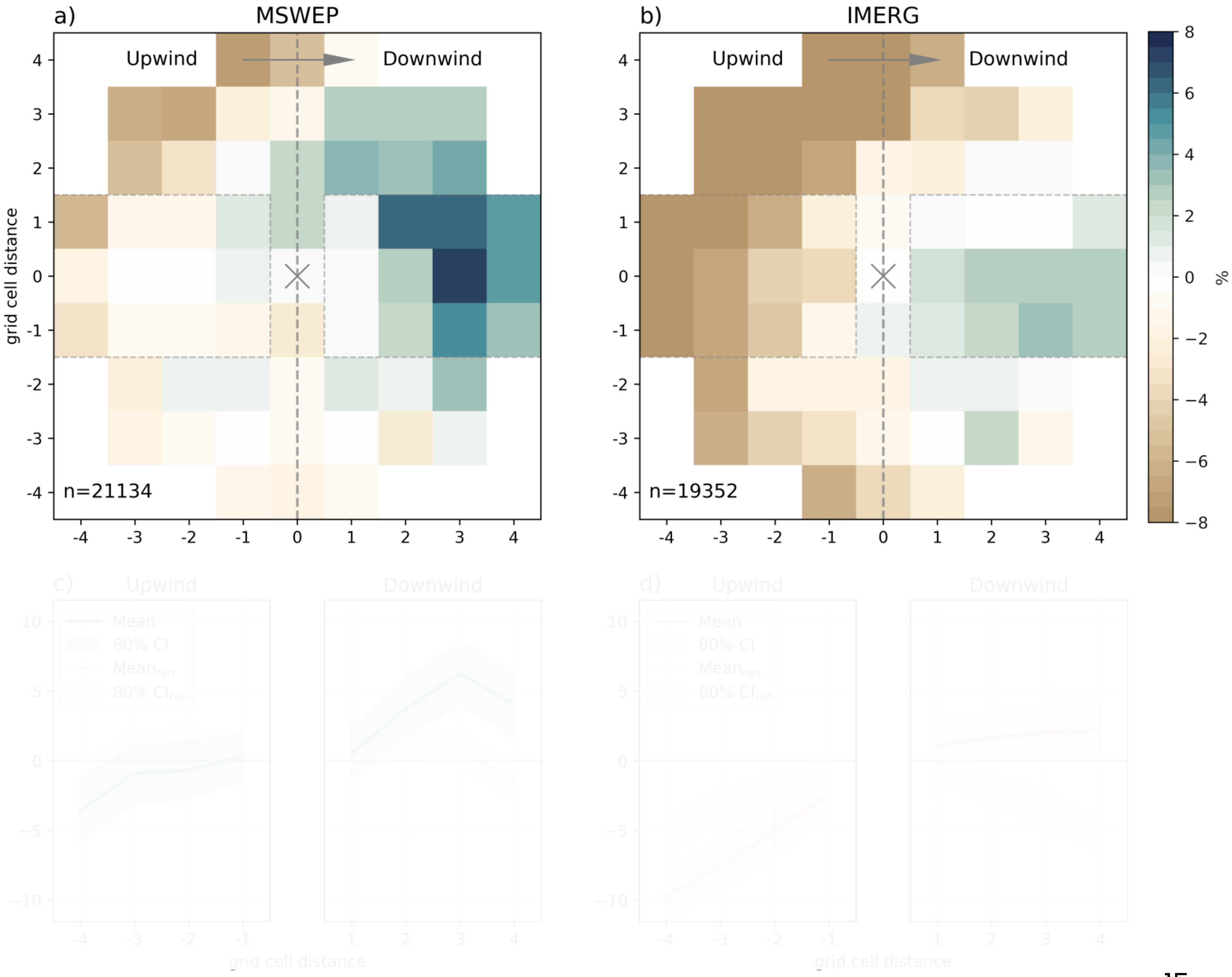

Afternoon rainfall likelihood

- Enhanced likelihood of afternoon rain 10km to 50km downwind of irrigated areas
- Signal emerges from the confidence interval obtained from randomly sampling wind directions

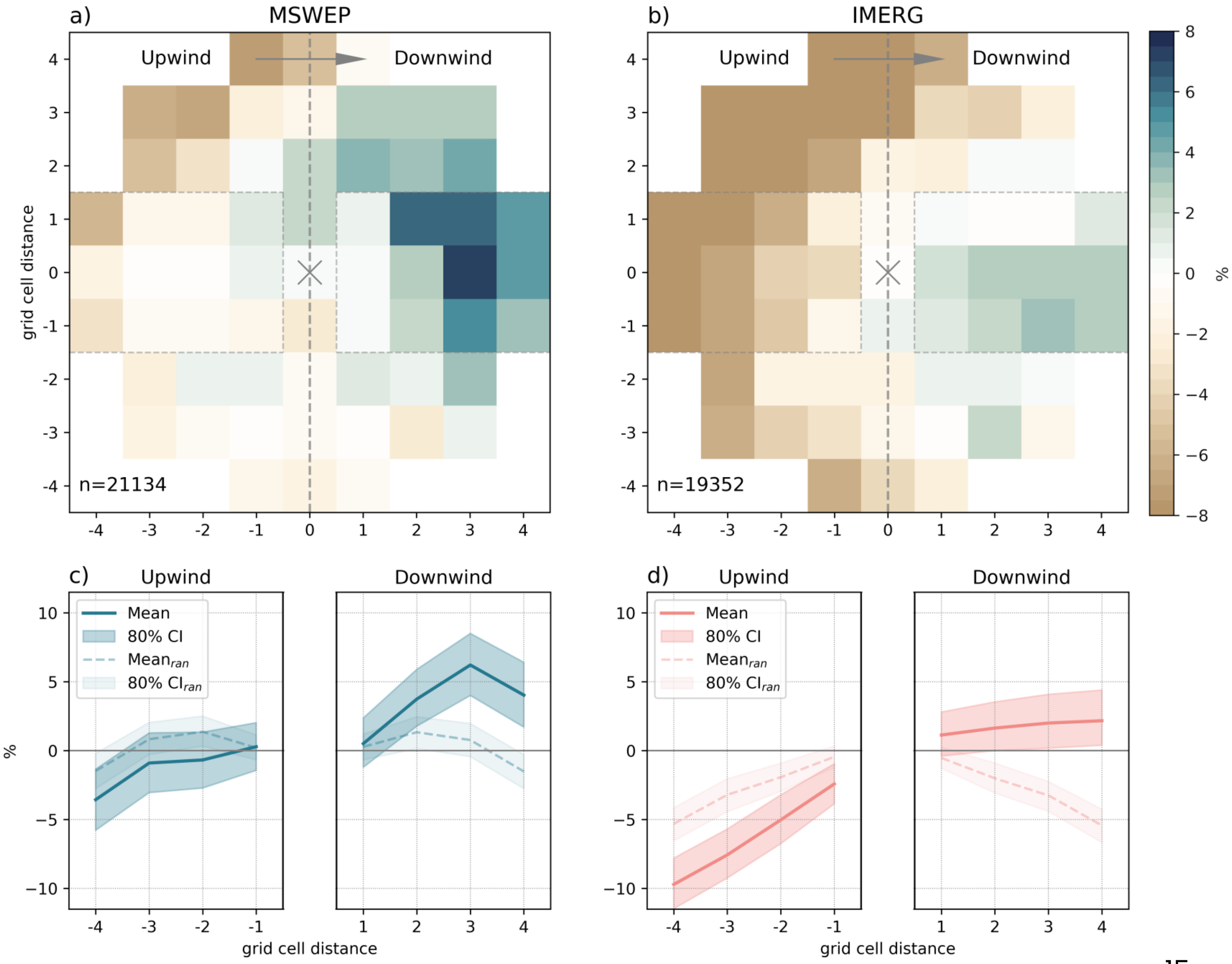

Regional signal

2001–2020

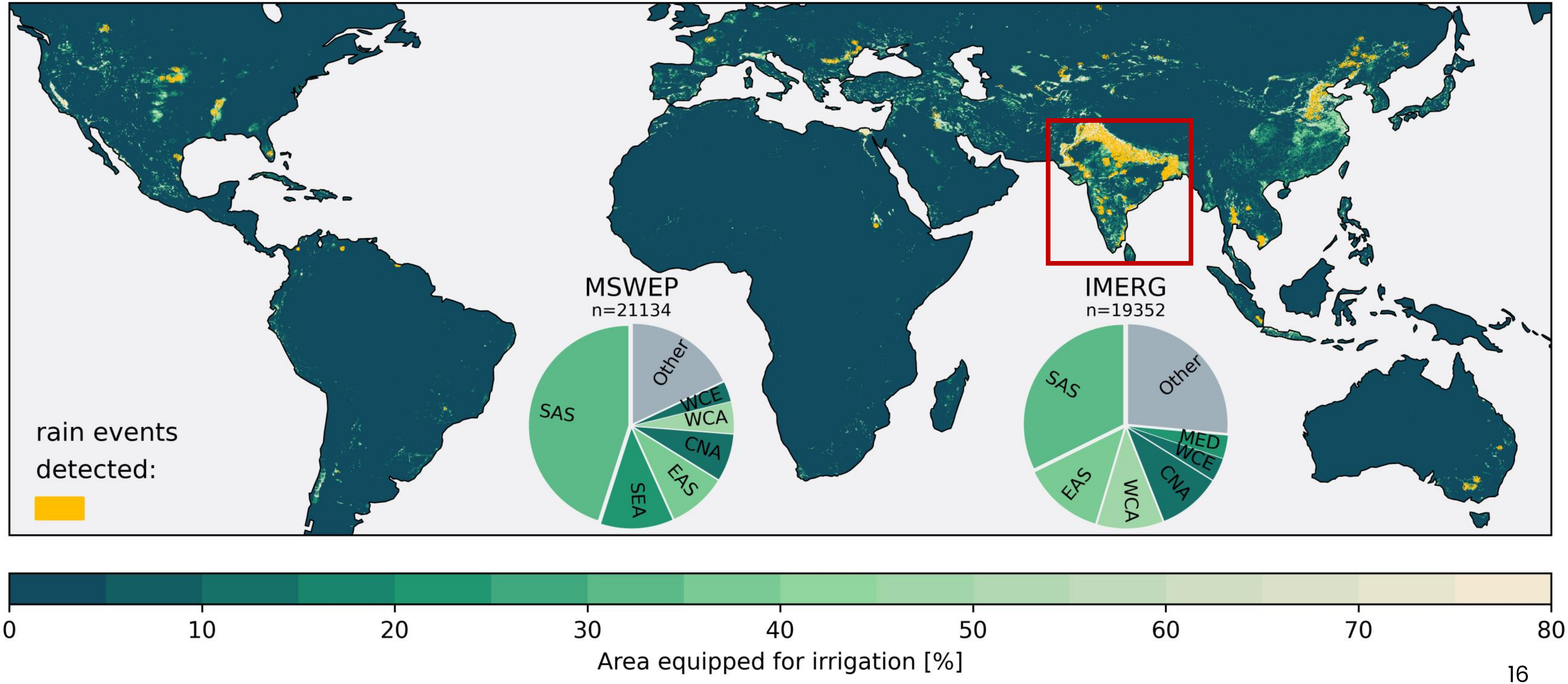

Regional signals

- Global signal is not dominated by irrigation-rainfall interactions in South Asia

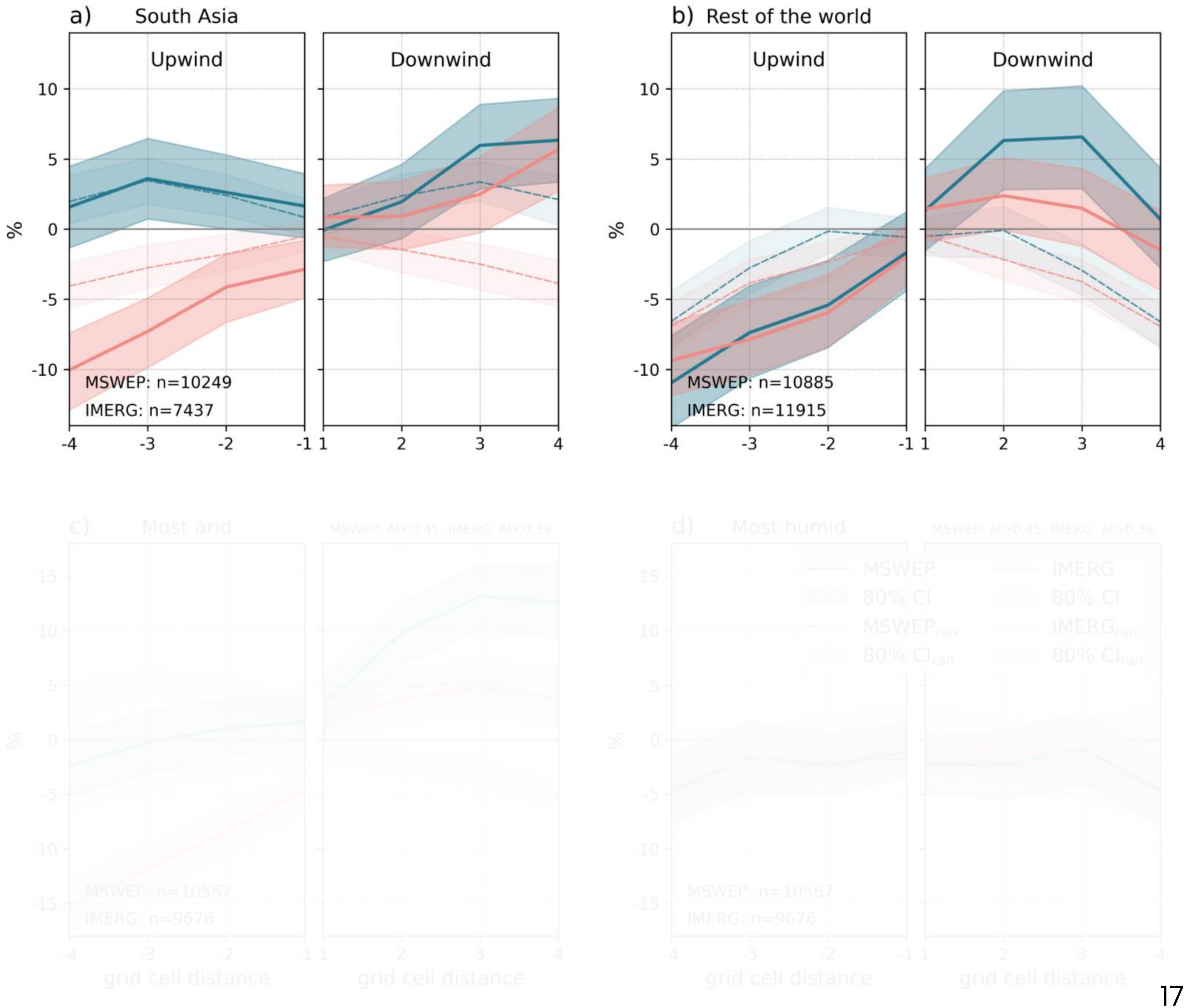

Regional signals

- Global signal is not dominated by irrigation-rainfall interactions in South Asia
- Signal is stronger under more arid conditions and almost disappears under humid conditions

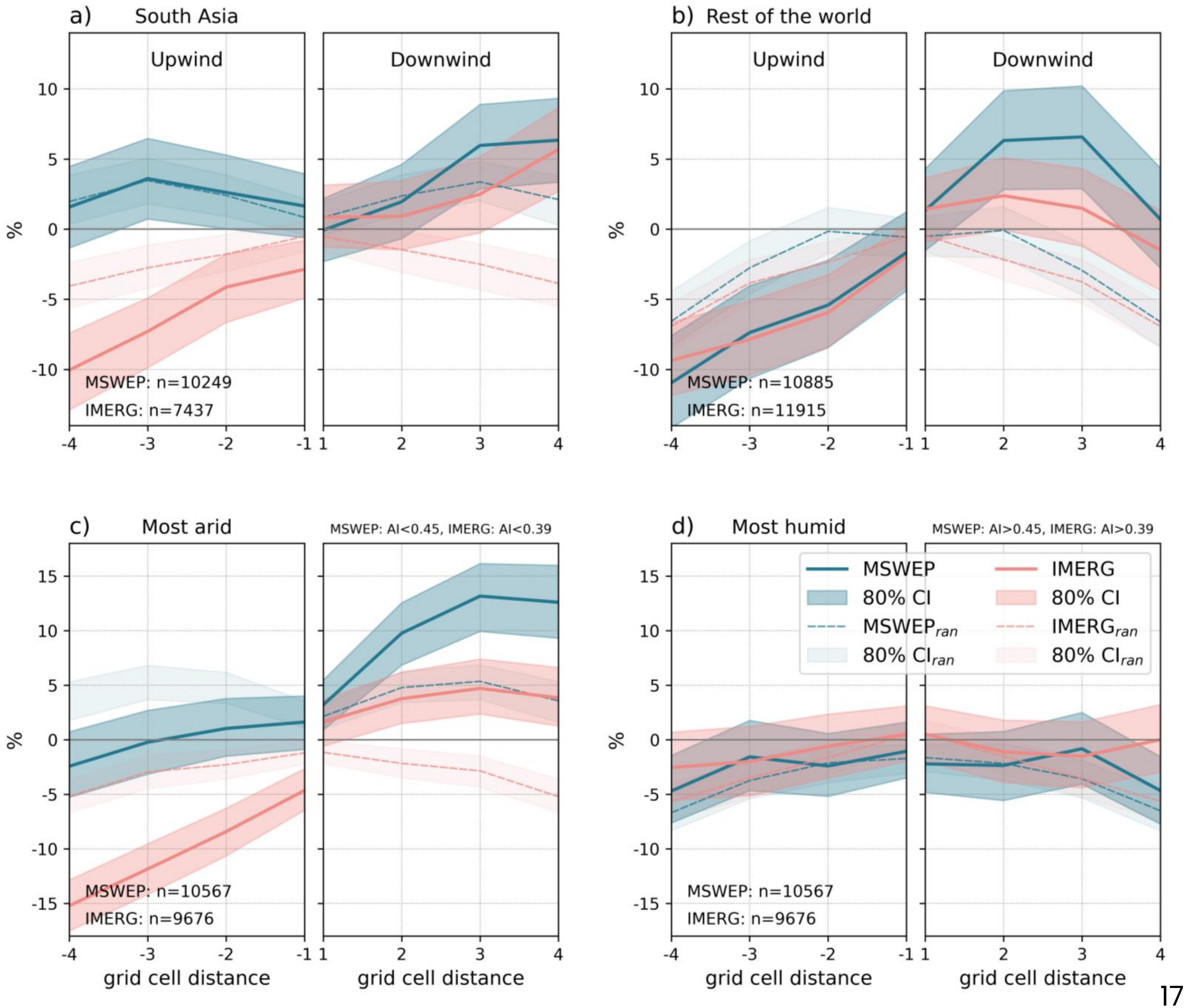

Irrigation influence

- When lowering the irrigation threshold, the detected downwind signal vanishes

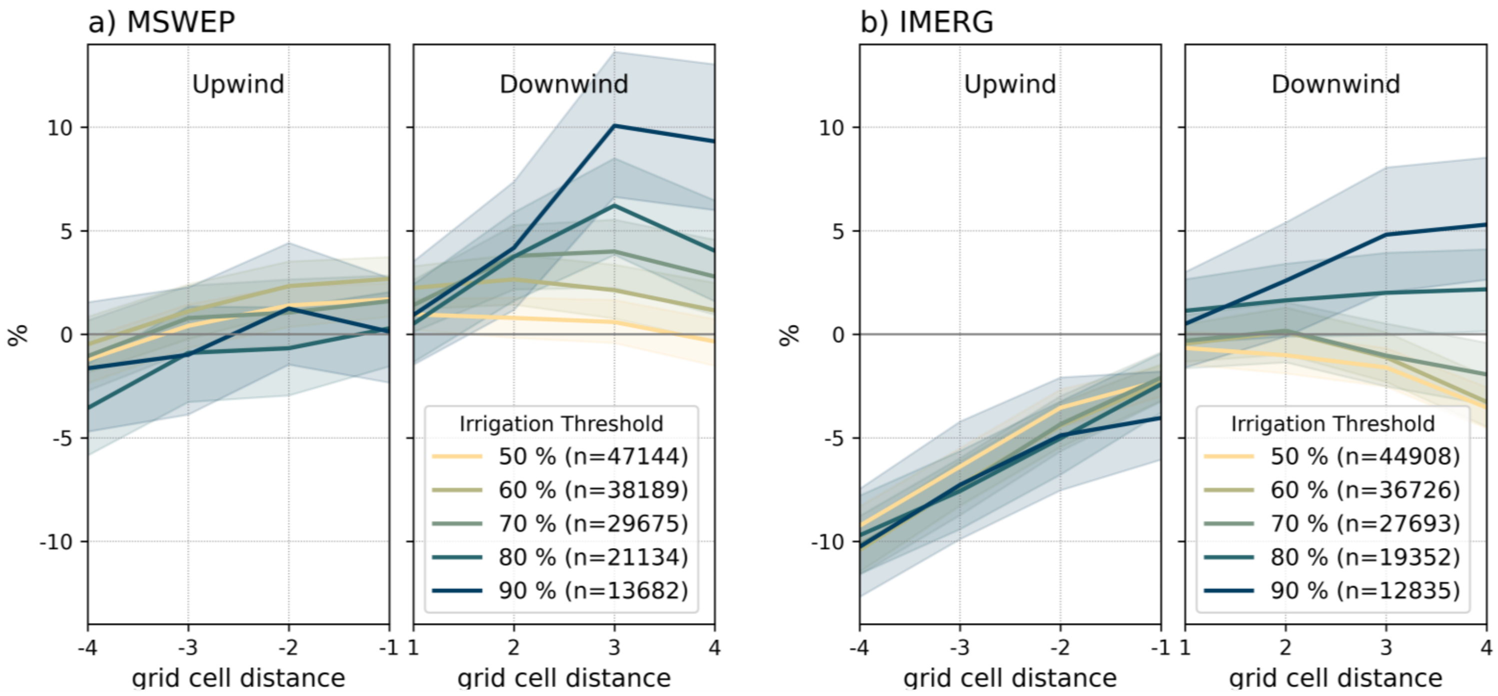

Downwind peak in signal

- When lowering the irrigation threshold, the detected downwind signal vanishes
- Extending the radius to 70km shows that the signal peaks between 30km to 50km downwind

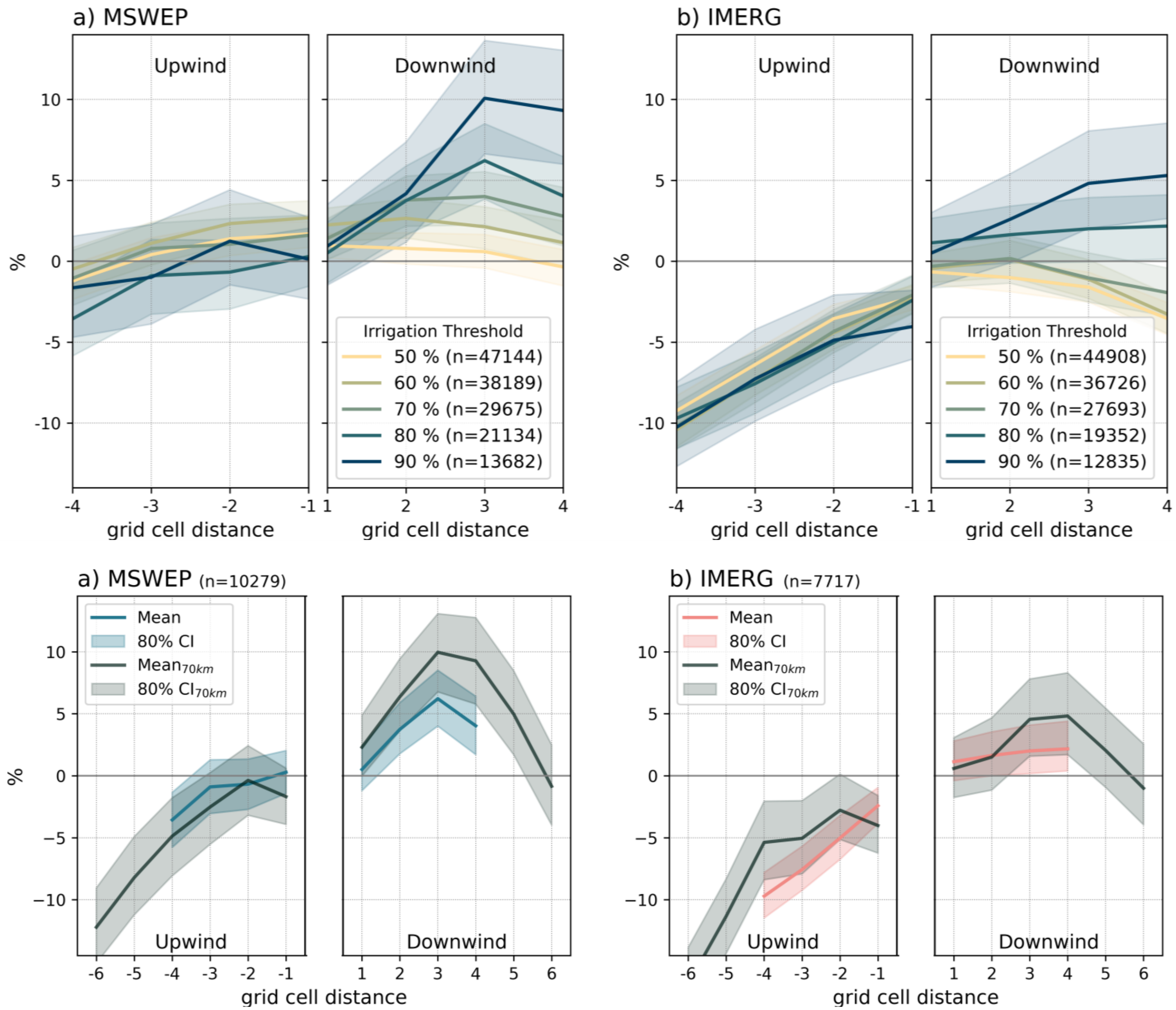

Possible mechanisms

Upwind

- Impact of upwind irrigation unclear
- Possible impact due to changes in mesoscale circulation patterns

Irrigated land

- Enhanced latent heat flux
- Reduced daytime near-surface warming
- Shallower and more stable boundary layer

Downwind

- Unhindered boundary layer growth

1. Daytime moist air advection may increase vertical mixing
2. Nighttime moisture advection -> early, more rapid boundary layer growth

Higher potential for deep convection?

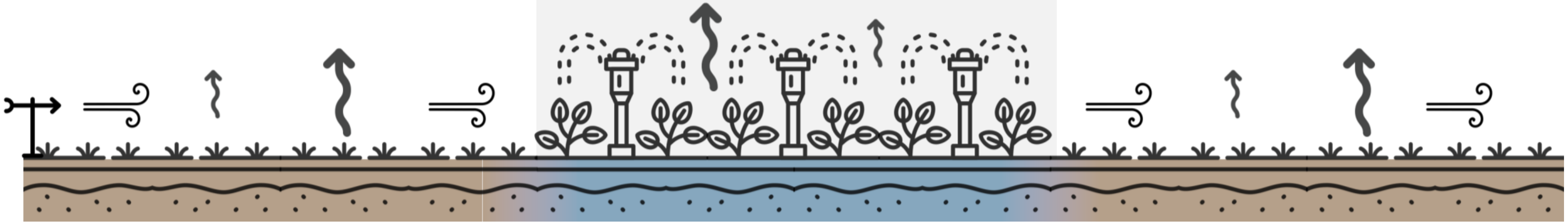

Impact on total afternoon rain amount

- Q-Q plots of afternoon rain amount between downwind and non-downwind regions
- Non-downwind rain events show slightly higher rain amounts for the strongest rain events (Q90 and above)

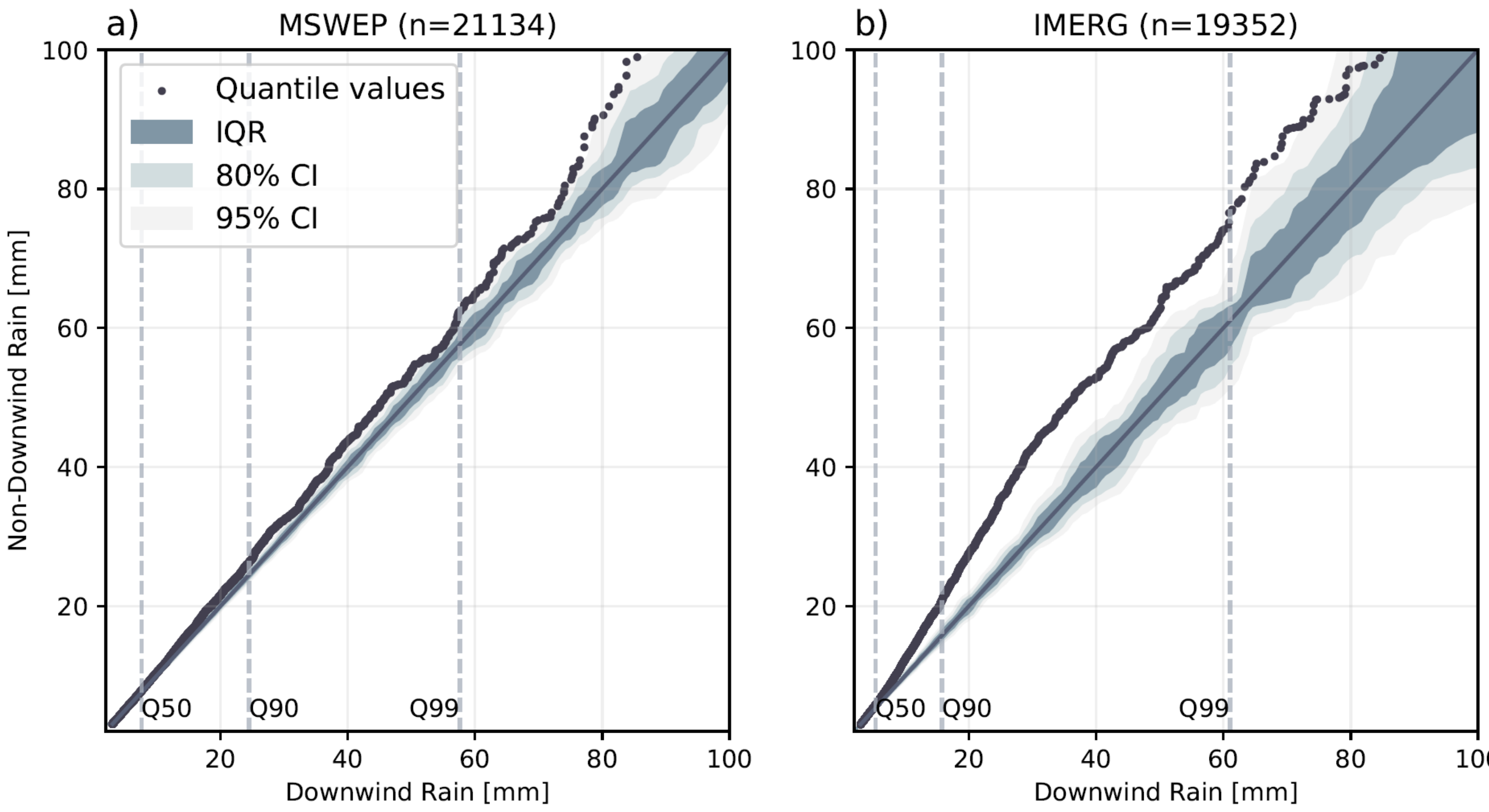

Impact on total afternoon rain amount

- Q-Q plots of afternoon rain amount between downwind and non-downwind regions
- Non-downwind rain events show slightly higher rain amounts for the strongest rain events (Q90 and above)

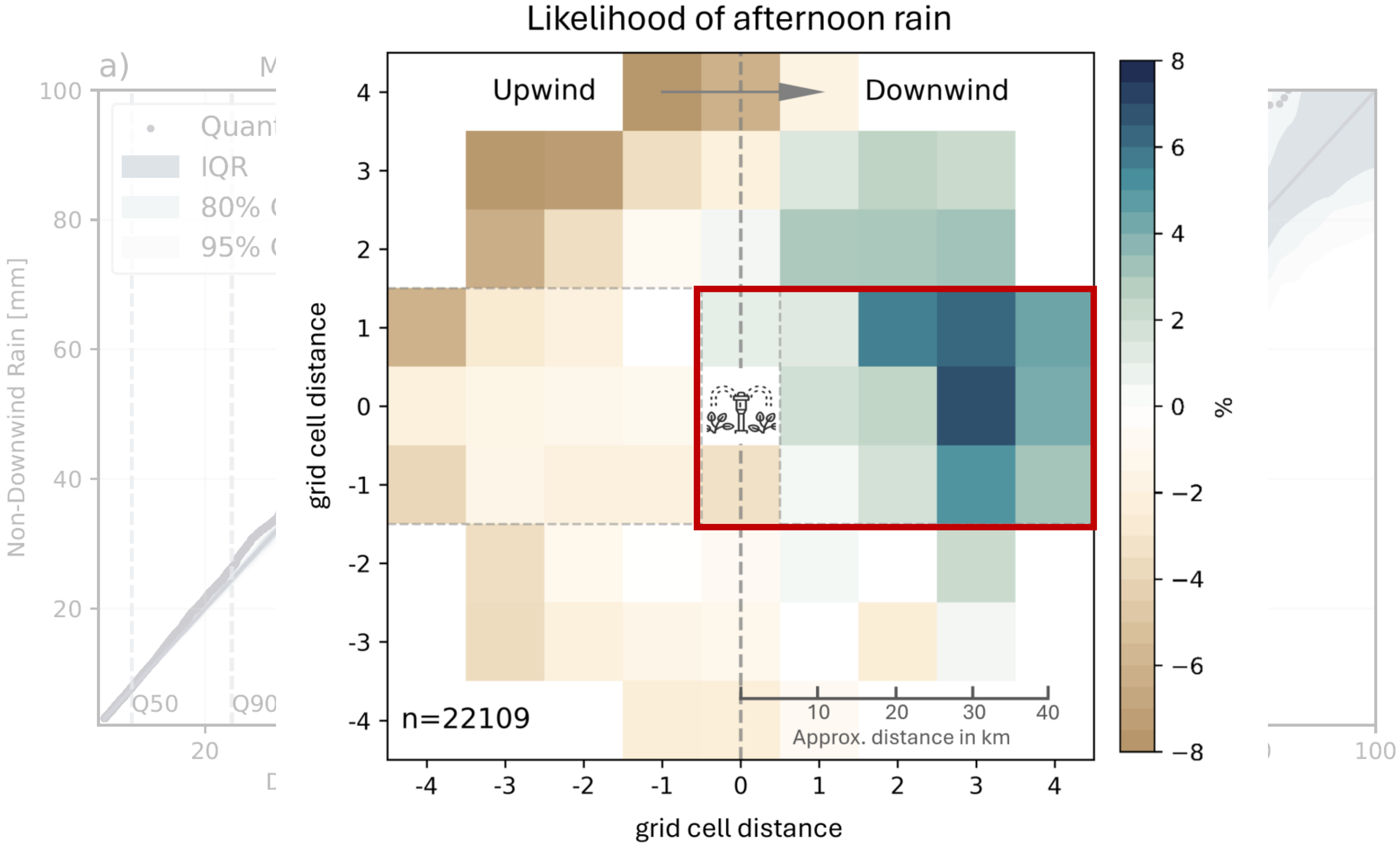

Impact on total afternoon rain amount

- Q-Q plots of afternoon rain amount between downwind and non-downwind regions
- Non-downwind rain events show slightly higher rain amounts for the strongest rain events (Q90 and above)

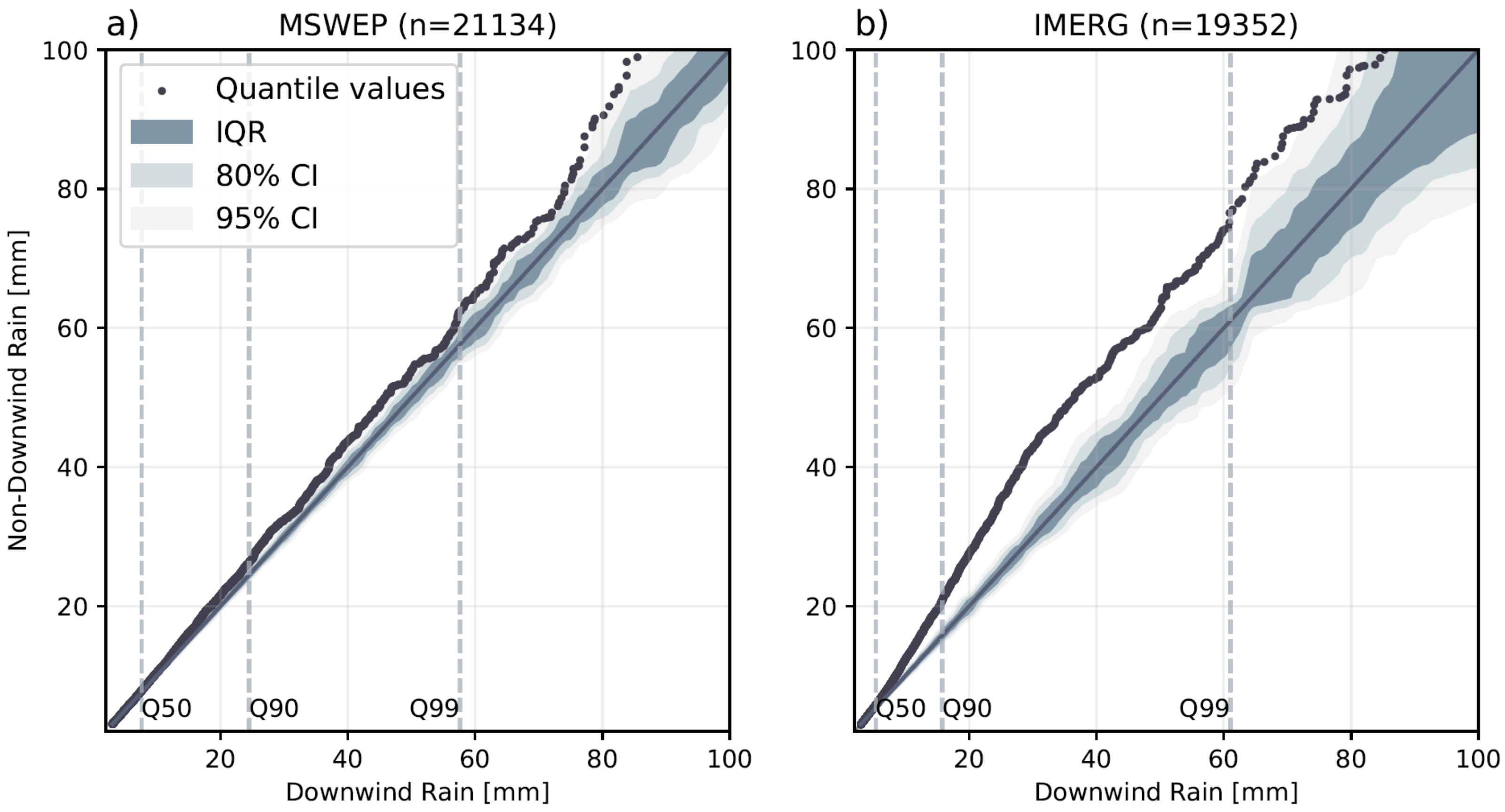

Summary

Our analysis detects a robust global signal on the impact of irrigation on local afternoon rainfall

- Large-scale irrigation enhances the likelihood of afternoon rain 10km to 50km downwind of irrigated areas
- Results can help to constrain newest models that represent irrigation and provide new insights into irrigation water management

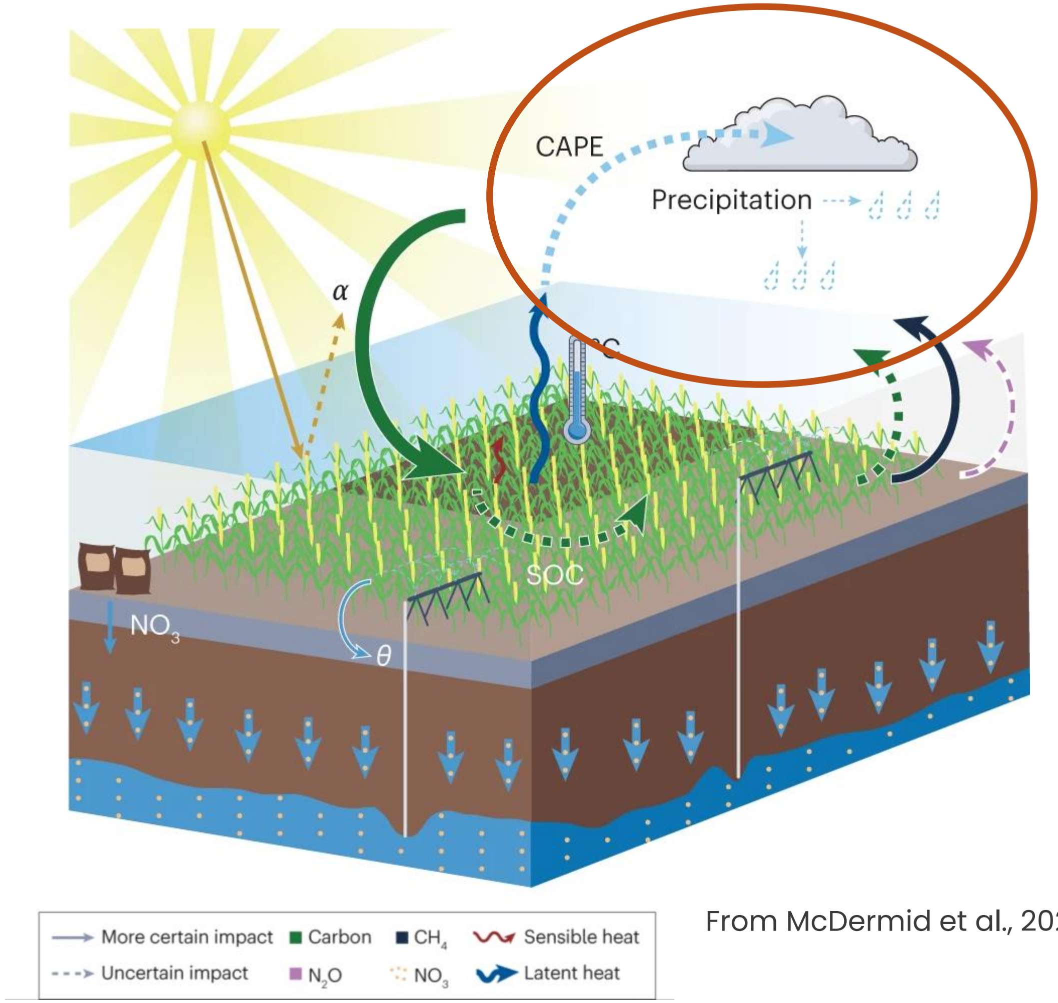

From McDermid et al., 2023

Thank you!

Greve, P.; Schmitt, A.; Miralles, D.; McDermid, S.; Findell, K.; García-García, A.; Peng, J. (2025): Observational evidence of increased afternoon rainfall downwind of irrigated areas. *Nature Communications* **16**, 3415

Job offer

PhD position on Global irrigation-atmosphere interaction

Supplementary Plots

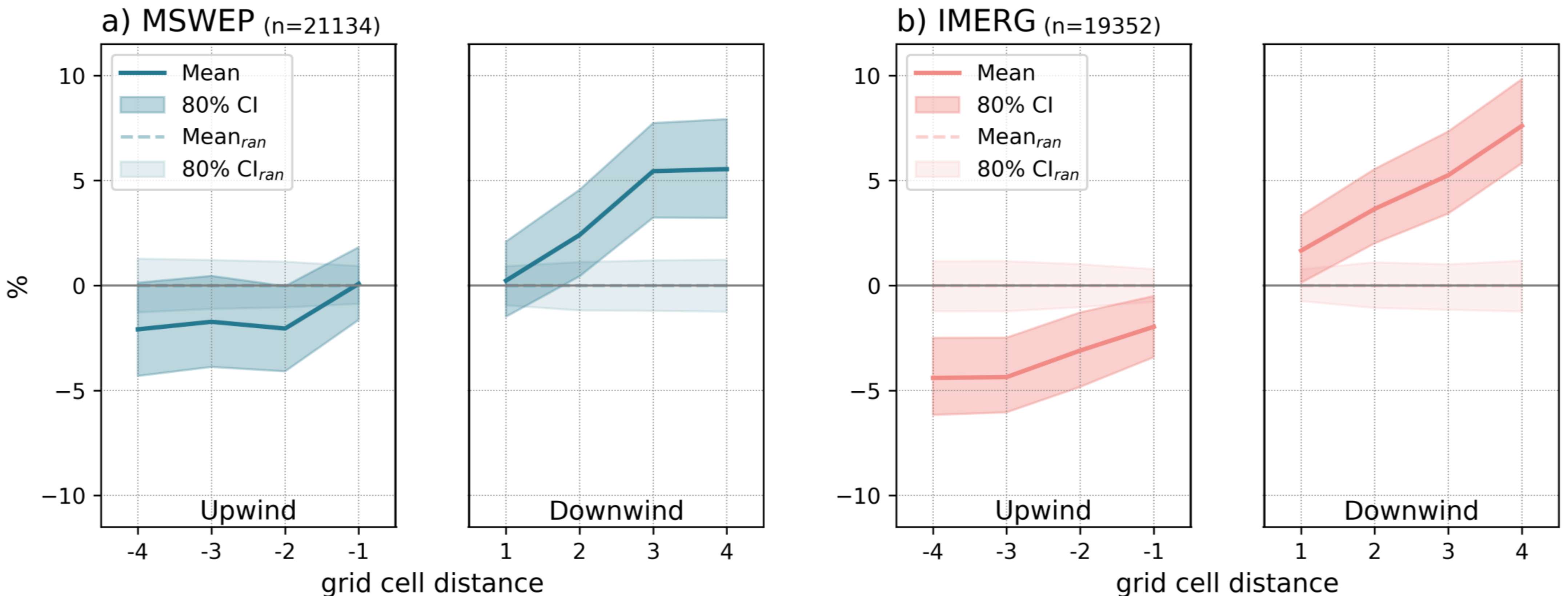

Average likelihood of peak afternoon rain along the wind direction normalized by randomized wind directions. This means that the average of the randomized wind directions is subtracted from the average likelihood and 80% confidence interval (shaded area). The dashed line (zero due to normalization) and the pale shading indicate the average and the 80% CI for the randomized wind directions (CI_ran).

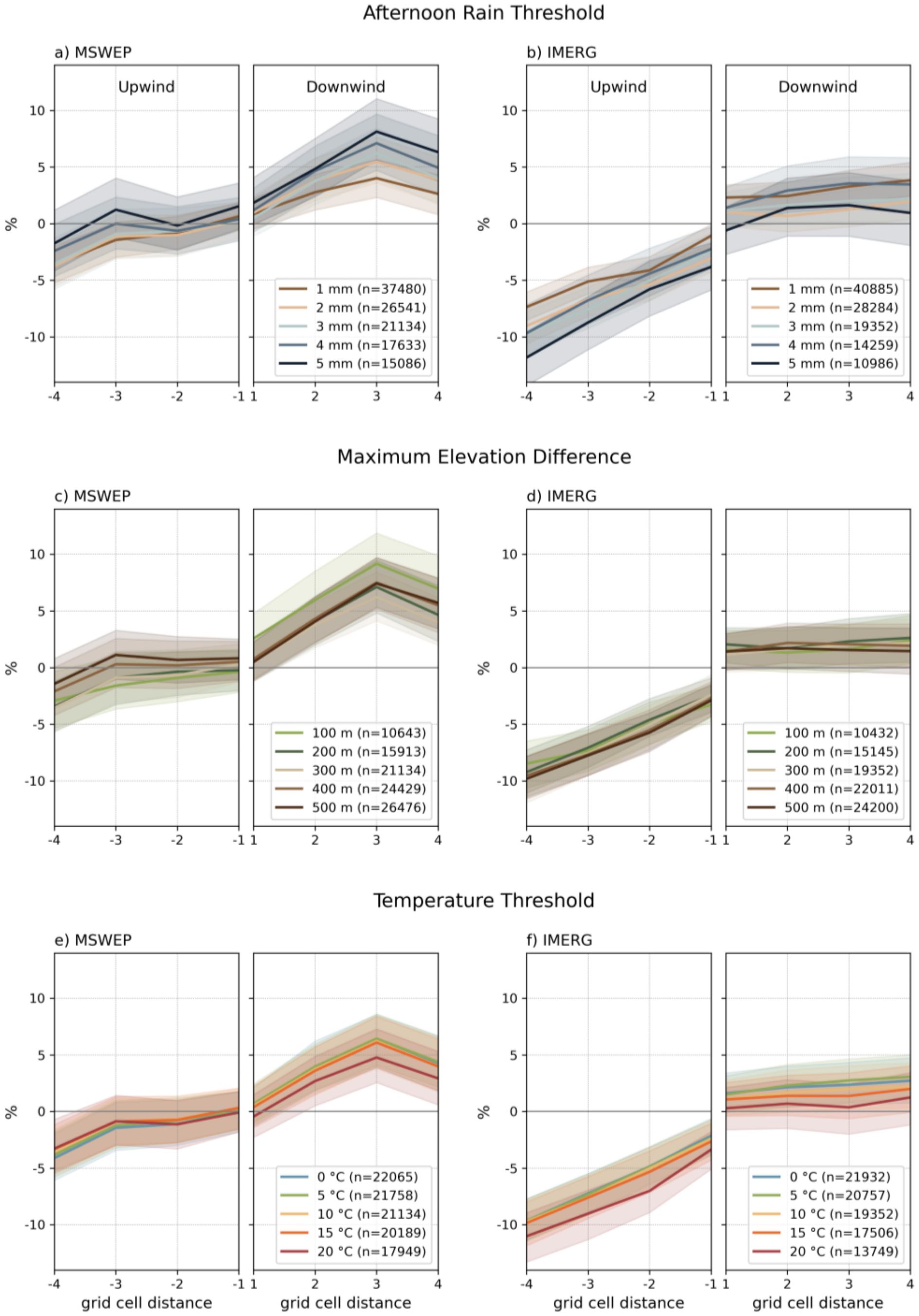

Average likelihood of irrigated grid cells along the wind direction for MSWEP and IMERG rain data under varying afternoon rain thresholds (a,b), maximum elevation differences (c,d), and temperature thresholds (e,f). The shaded areas represent the 80% confidence interval (CI) based on a bootstrapping approach.

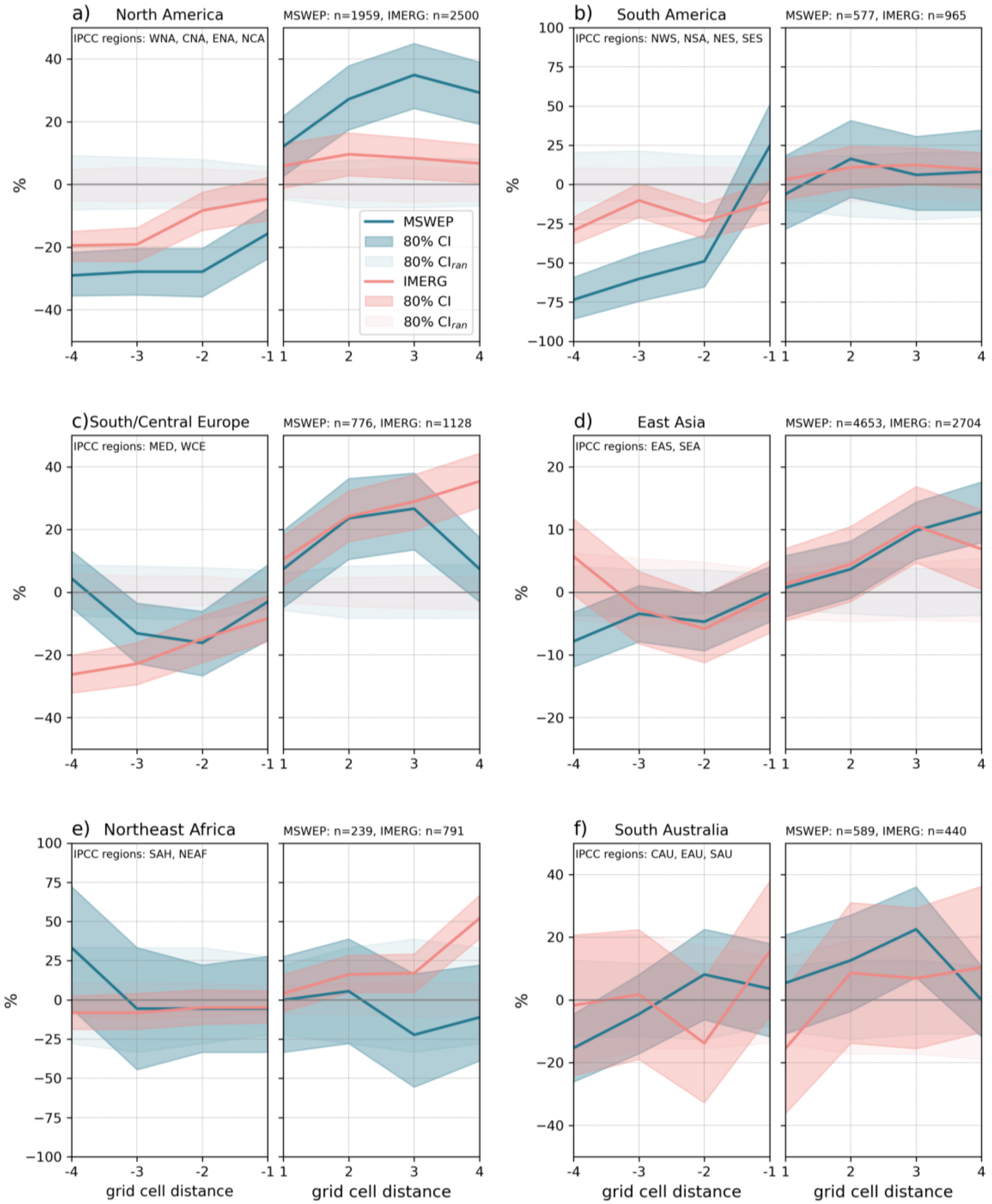

Regional differences in peak rainfall likelihood: Average likelihood of peak afternoon rain along the wind direction normalized by randomized wind directions for rain events detected in (a) North America, (b) South America, (c) South/Central Europe, (d) East Asia, (e) Northeast Africa and (f) South Australia. The shaded area represents the 80% confidence interval (CI) based on a bootstrapping approach. The dashed line (zero due to normalization) and the pale shading indicate the average and the 80% CI for the randomized wind directions (CI_ran). Please note that the sample sizes, detected relative differences, and their associated uncertainties vary between the regions (note the different y-axes).

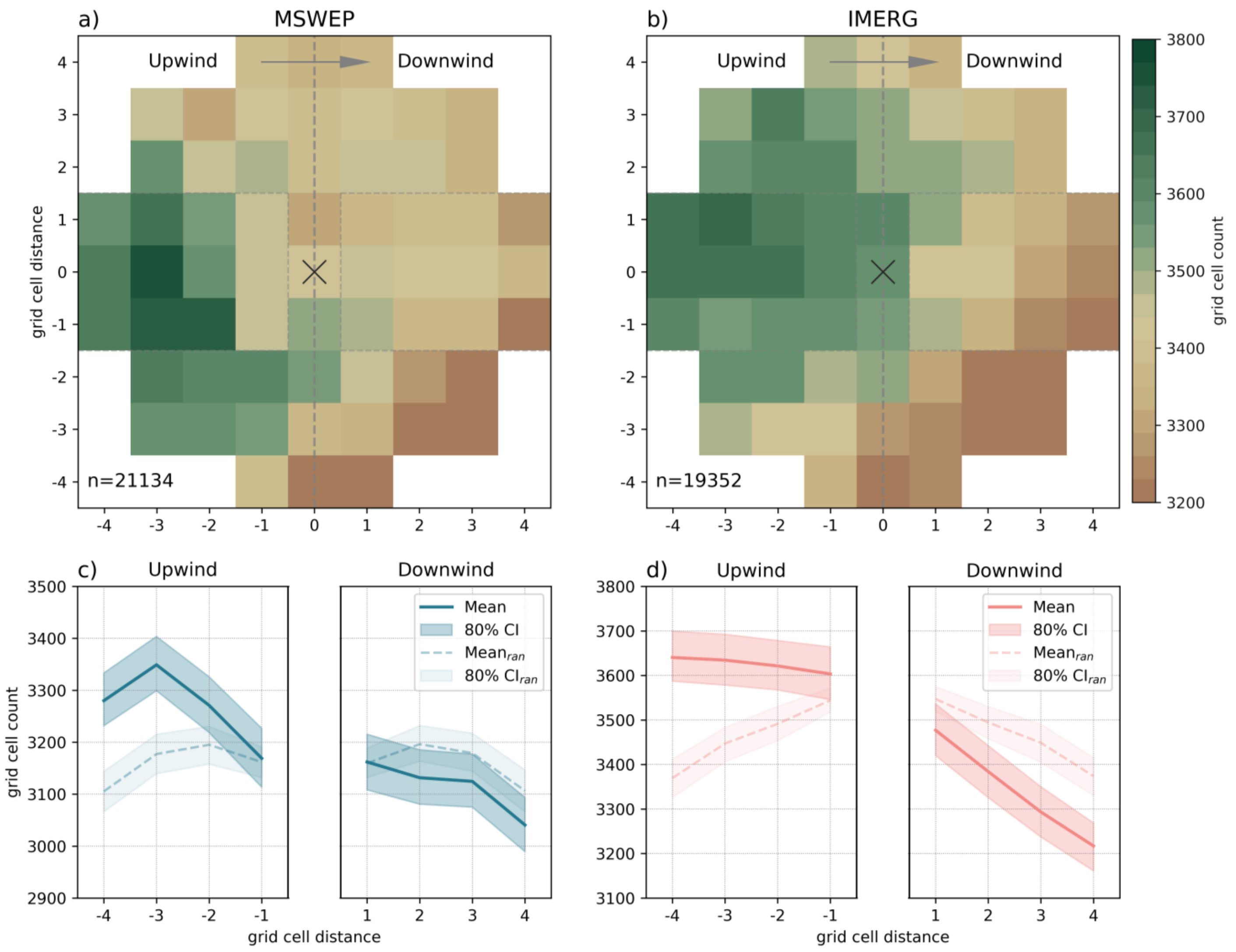

Sum of irrigated grid cells across all rain events relative to the location of peak afternoon rain. (a, b) Raster maps showing the sum of irrigated grid cells relative to the location of peak afternoon rain centred at (0,0) for MSWEP and IMERG rain data. Wind direction is normalized such that upwind (downwind) areas are on the left (right). In comparison to Fig. 3within this reference system centred around the peak afternoon rain location, grid locations to the left of the centre define areas upwind of peak afternoon rainfall, i.e., the peak location is located downwind of these areas. Similarly, grid locations to the right of the centre define areas downwind of peak afternoon rainfall, i.e., the peak rain location is located upwind of these areas. (c, d) Average sum of irrigated grid cells along the wind direction (+/-1 grid cells, within the dashed horizontal lines in a, b). The shaded area represents the 80% confidence interval (CI) based on a bootstrapping approach. The dashed line and the pale shading indicate the average and the 80% CI for the randomized wind directions (CI_ran).